induced vascular stabilization by inhibiting VEGF-mediated internalization of vascular endothelial cadherin resulted in suppression of hind limb oedema (*61*). In addition to its role in blood vessel formation, APJ is expressed in human lymphatic ECs, and apelin induces their migration and cord formation. Transgenic mice harbouring apelin in the dermis showed reduced development of oedema by promoting stabilization of lymphatic vessels (*63*). Taken together, these findings suggest that the apelin/APJ system represents a new therapeutic target for ischaemic disease.

Conclusions

Recent studies have revealed multiple roles of the apelin/APJ system in vascular formation in physiological and pathological situations, including during development, tissue regeneration and tumourigenesis. Apelin has a unique function as a regulator of vascular maturation and stabilization by increasing the caliber of newly formed blood vessels and strengthening barrier function between ECs. Moreover, expression of apelin and APJ genes is temporally upregulated during blood vessel development and downregulated in stabilized vasculature. Detailed understanding of the function of the apelin/APJ system and expression analysis in blood vessels will provide insights for improving the use of agonists and antagonists that modulate apelin signalling in different vascular diseases.

Funding
This work was supported by Grant-in Aid for Scientific Research on Innovative Areas (No. 23122511) from the Ministry of Education, Culture, Sports, Science and Technology (MEXT) and Grant-in Aid for Young Scientist B (No. 23701054) from the Japan Society for the Promotion of Science (JSPS).

Conflict of interest
None declared.

References

1. Tatemoto, K., Hosoya, M., Habata, Y., Fujii, R., Kakegawa, T., Zou, M.X., Kawamata, Y., Fukusumi, S., Hinuma, S., Kitada, C., Kurokawa, T., Onda, H., and Fujino, M. (1998) Isolation and characterization of a novel endogenous peptide ligand for the human APJ receptor. *Biochem. Biophys. Res. Commun.* **251**, 471–476
2. Kawamata, Y., Habata, Y., Fukusumi, S., Hosoya, M., Fujii, R., Hinuma, S., Nishizawa, N., Kitada, C., Onda, H., Nishimura, O., and Fujino, M. (2001) Molecular properties of apelin: tissue distribution and receptor binding. *Biochim. Biophys. Acta.* **1538**, 162–171
3. Masri, B., Lahlou, H., Mazarguil, H., Knibiehler, B., and Audigier, Y. (2002) Apelin (65-77) activates extracellular signal-regulated kinases via a PTX-sensitive G protein. *Biochem. Biophys. Res. Commun.* **290**, 539–545
4. Lee, D.K., Ferguson, S.S., George, S.R., and O'Dowd, B.F. (2010) The fate of the internalized apelin receptor is determined by different isoforms of apelin mediating differential interaction with beta-arrestin. *Biochem. Biophys. Res. Commun.* **395**, 185–189
5. O'Dowd, B.F., Heiber, M., Chan, A., Heng, H.H., Tsui, L.C., Kennedy, J.L., Shi, X., Petronis, A., George, S.R., and Nguyen, T. (1993) A human gene that shows identity with the gene encoding the angiotensin receptor is located on chromosome 11. *Gene* **136**, 355–360
6. Lee, D.K., Cheng, R., Nguyen, T., Fan, T., Kariyawasam, A.P., Liu, Y., Osmond, D.H., George, S.R., and O'Dowd, B.F. (2000) Characterization of apelin, the ligand for the APJ receptor. *J. Neurochem.* **74**, 34–41
7. Tatemoto, K., Takayama, K., Zou, M.X., Kumaki, I., Zhang, W., Kumano, K., and Fujimiya, M. (2001) The novel peptide apelin lowers blood pressure via a nitric oxide-dependent mechanism. *Regul. Pept.* **99**, 87–92
8. Katugampola, S.D., Maguire, J.J., Matthewson, S.R., and Davenport, A.P. (2001) [(125)I]-(Pyr(1))Apelin-13 is a novel radioligand for localizing the APJ orphan receptor in human and rat tissues with evidence for a vasoconstrictor role in man. *Br. J. Pharmacol.* **132**, 1255–1260
9. Foldes, G., Horkay, F., Szokodi, I., Vuolteenaho, O., Ilves, M., Lindstedt, K.A., Mäyränpää, M., Sármán, B., Seres, L., Skoumal, R., Lakó-Futó, Z., deChâtel, R., Ruskoaho, H., and Tóth, M. (2003) Circulating and cardiac levels of apelin, the novel ligand of the orphan receptor APJ, in patients with heart failure. *Biochem. Biophys. Res. Commun.* **308**, 480–485
10. Ronkainen, V.P., Ronkainen, J.J., Hanninen, S.L., Leskinen, H., Ruas, J.L., Pereira, T., Poellinger, L., Vuolteenaho, O., and Tavi, P. (2007) Hypoxia inducible factor regulates the cardiac expression and secretion of apelin. *FASED J.* **21**, 1821–1830
11. Berry, M.F., Pirolli, T.J., Jayasankar, V., Burdick, J., Morine, K.J., Gardner, T.J., and Woo, Y.J. (2004) Apelin has in vivo inotropic effects on normal and failing hearts. *Circulation* **110 (11 Suppl. 1)**, II187–II193
12. Jia, Y.X., Pan, C.S., Zhang, J., Geng, B., Zhao, J., Gerns, H., Yang, J., Chang, J.K., Tang, C.S., and Qi, Y.F. (2006) Apelin protects myocardial injury induced by isoproterenol in rats. *Regul. Pept.* **133**, 147–154
13. Atluri, P., Morine, K.J., Liao, G.P., Panlilio, C.M., Berry, M.F., Hsu, V.M., Hiesinger, W., Cohen, J.E., and Joseph Woo, Y. (2007) Ischemic heart failure enhances endogenous myocardial apelin and APJ receptor expression. *Cell. Mol. Biol. Lett.* **12**, 127–138
14. Maguire, J.J., Kleinz, M.J., Pitkin, S.L., and Davenport, A.P. (2009) [Pyr1]apelin-13 identified as the predominant apelin isoform in the human heart: vasoactive mechanisms and inotropic action in disease. *Hypertension* **54**, 598–604
15. Boucher, J., Masri, B., Daviaud, D., Gesta, S., Guigne, C., Mazzucotelli, A., Castan-Laurell, I., Tack, I., Knibiehler, B., Carpéné, C., Audiqier, Y., Saulnier-Blanche, J.S., and Valet, P. (2005) Apelin, a newly identified adipokine up-regulated by insulin and obesity. *Endocrinology* **146**, 1764–1771
16. Heinonen, M.V., Purhonen, A.K., Miettinen, P., Paakkonen, M., Pirinen, E., Alhava, E., Akerman, K., and Herzig, K.H. (2005) Apelin, orexin-A and leptin plasma levels in morbid obesity and effect of gastric banding. *Regul. Pept.* **130**, 7–13
17. Li, L., Yang, G., Li, Q., Tang, Y., Yang, M., Yang, H., and Li, K. (2006) Changes and relations of circulating visfatin, apelin, and resistin levels in normal, impaired glucose tolerance, and type 2 diabetic subjects. *Exp. Clin. Endocrinol. Diabetes* **114**, 544–548

18. Roberts, E.M., Newson, M.J., Pope, G.R., Landgraf, R., Lolait, S.J., and O'Carroll, A.M. (2009) Abnormal fluid homeostasis in apelin receptor knockout mice. *J. Endocrinol.* **202**, 453–462
19. Lambrecht, N.W., Yakubov, I., Zer, C., and Sachs, G. (2006) Transcriptomes of purified gastric ECL and parietal cells: identification of a novel pathway regulating acid secretion. *Physiol. Genomics* **25**, 153–165
20. Habata, Y., Fujii, R., Hosoya, M., Fukusumi, S., Kawamata, Y., Hinuma, S., Kitada, C., Nishizawa, N., Murosaki, S., Kurokawa, T., Onda, H., Tatemoto, K., and Fujino, M. (1999) Apelin, the natural ligand of the orphan receptor APJ, is abundantly secreted in the colostrum. *Biochim. Biophys. Acta.* **1452**, 25–35
21. Hosoya, M., Kawamata, Y., Fukusumi, S., Fujii, R., Habata, Y., Hinuma, S., Kitada, C., Honda, S., Kurokawa, T., Onda, H., Nishimura, O., and Fujino, M. (2000) Molecular and functional characteristics of APJ. Tissue distribution of mRNA and interaction with the endogenous ligand apelin. *J. Biol. Chem.* **275**, 21061–21067
22. O'Carroll, A.M., Selby, T.L., Palkovits, M., and Lolait, S.J. (2000) Distribution of mRNA encoding B78/apj, the rat homologue of the human APJ receptor, and its endogenous ligand apelin in brain and peripheral tissues. *Biochim. Biophys. Acta.* **1492**, 72–80
23. Devic, E., Rizzoti, K., Bodin, S., Knibiehler, B., and Audigier, Y. (1999) Amino acid sequence and embryonic expression of msr/apj, the mouse homolog of Xenopus X-msr and human APJ. *Mech. Dev.* **84**, 199–203
24. Medhurst, A.D., Jennings, C.A., Robbins, M.J., Davis, R.P., Ellis, C., Winborn, K.Y., Lawrie, K.W., Hervieu, G., Riley, G., Bolaky, J.E., Herrity, N.C., Murdock, P., and Darker, J.G. (2003) Pharmacological and immunohistochemical characterization of the APJ receptor and its endogenous ligand apelin. *J. Neurochem.* **84**, 1162–1172
25. Edinger, A.L., Hoffman, T.L., Sharron, M., Lee, B., Yi, Y., Choe, W., Kolson, D.L., Mitrovic, B., Zhou, Y., Faulds, D., Collman, R.G., Hesselgesser, J., Horuk, R., and Doms, R.W. (1998) An orphan seven-transmembrane domain receptor expressed widely in the brain functions as a coreceptor for human immunodeficiency virus type 1 and simian immunodeficiency virus. *J. Virol.* **72**, 7934–7940
26. Kleinz, M.J. and Davenport, A.P. (2004) Immunocytochemical localization of the endogenous vasoactive peptide apelin to human vascular and endocardial endothelial cells. *Regul. Pept.* **118**, 119–125
27. Wang, G., Qi, X., Wei, W., Englander, E.W., and Greeley, G.H. Jr (2006) Characterization of the 5′-regulatory regions of the rat and human apelin genes and regulation of breast apelin by USF. *FASEB J.* **20**, 2639–2641
28. Han, S., Wang, G., Qi, X., Englander, E.W., and Greeley, G.H. Jr (2008) Involvement of a Stat3 binding site in inflammation-induced enteric apelin expression. *Am. J. Physiol. Gastrointest. Liver Physiol.* **295**, G1068–G1078
29. Mazzucotelli, A., Ribet, C., Castan-Laurell, I., Daviaud, D., Guigne, C., Langin, D., and Valet, P. (2008) The transcriptional co-activator PGC-1alpha up regulates apelin in human and mouse adipocytes. *Regul. Pept.* **150**, 33–37
30. Eyries, M., Siegfried, G., Ciumas, M., Montagne, K., Agrapart, M., Lebrin, F., and Soubrier, F. (2008) Hypoxia-induced apelin expression regulates endothelial cell proliferation and regenerative angiogenesis. *Circ. Res.* **103**, 432–440
31. O'Carroll, A.M., Lolait, S.J., and Howell, G.M. (2006) Transcriptional regulation of the rat apelin receptor gene: promoter cloning and identification of an Sp1 site necessary for promoter activity. *J. Mol. Endocrinol.* **36**, 221–235
32. Hata, J., Matsuda, K., Ninomiya, T., Yonemoto, K., Matsushita, T., Ohnishi, Y., Saito, S., Kitazono, T., Ibayashi, S., Iida, M., Kiyohara, Y., Nakamura, Y., and Kubo, M. (2007) Functional SNP in an Sp1-binding site of AGTRL1 gene is associated with susceptibility to brain infarction. *Hum. Mol. Genet.* **16**, 630–639
33. Kasai, A., Shintani, N., Oda, M., Kakuda, M., Hashimoto, H., Matsuda, T., Hinuma, S., and Baba, A. (2004) Apelin is a novel angiogenic factor in retinal endothelial cells. *Biochem. Biophys. Res. Commun.* **325**, 395–400
34. Hashimoto, Y., Ishida, J., Yamamoto, R., Fujiwara, K., Asada, S., Kasuya, Y., Mochizuki, N., and Fukamizu, A (2005) G protein-coupled APJ receptor signaling induces focal adhesion formation and cell motility. *Int. J. Mol. Med* **16**, 787–792
35. Masri, B., Morin, N., Cornu, M., Knibiehler, B., and Audigier, Y. (2004) Apelin (65-77) activates p70 S6 kinase and is mitogenic for umbilical endothelial cells. *FASEB J.* **18**, 1909–1911
36. Li, Y., Chen, J., Bai, B., Du, H., Liu, Y., and Liu, H. (2012) Heterodimerization of human apelin and kappa opioid receptors: roles in signal transduction. *Cell. Signal.* **24**, 991–1001
37. Alastalo, T.P., Li, M., Perez Vde, J., Pham, D., Sawada, H., Wang, J.K., Koskenvuo, M., Wang, L., Freeman, B.A., Chang, H.Y., and Rabinovitch, M. (2011) Disruption of PPARgamma/beta-catenin-mediated regulation of apelin impairs BMP-induced mouse and human pulmonary arterial EC survival. *J. Clin. Invest.* **121**, 3735–3746
38. Xie, H., Yuan, L.Q., Luo, X.H., Huang, J., Cui, R.R., Guo, L.J., Zhou, H.D., Wu, X.P., and Liao, E.Y. (2007) Apelin suppresses apoptosis of human osteoblasts. *Apoptosis* **12**, 247–254
39. Masri, B., Morin, N., Pedebernade, L., Knibiehler, B., and Audigier, Y. (2006) The apelin receptor is coupled to Gi1 or Gi2 protein and is differentially desensitized by apelin fragments. *J. Biol. Chem.* **281**, 18317–18326
40. Risau, W. (1997) Mechanisms of angiogenesis. *Nature* **386**, 671–674
41. Kalin, R.E., Kretz, M.P., Meyer, A.M., Kispert, A., Heppner, F.L., and Brandli, A.W. (2007) Paracrine and autocrine mechanisms of apelin signaling govern embryonic and tumor angiogenesis. *Dev. Biol.* **305**, 599–614
42. Cox, C.M., D'Agostino, S.L., Miller, M.K., Heimark, R.L., and Krieg, P.A. (2006) Apelin, the ligand for the endothelial G-protein-coupled receptor, APJ, is a potent angiogenic factor required for normal vascular development of the frog embryo. *Dev. Biol.* **296**, 177–189
43. Tucker, B., Hepperle, C., Kortschak, D., Rainbird, B., Wells, S., Oates, A.C., and Lardelli, M. (2007) Zebrafish angiotensin II receptor-like 1a (agtrl1a) is expressed in migrating hypoblast, vasculature, and in multiple embryonic epithelia. *Gene Expr. Patterns* **7**, 258–265
44. Kidoya, H., Ueno, M., Yamada, Y., Mochizuki, N., Nakata, M., Yano, T., Fujii, R., and Takakura, N. (2008) Spatial and temporal role of the apelin/APJ

system in the caliber size regulation of blood vessels during angiogenesis. *EMBO J.* **27**, 522–534

45. Saint-Geniez, M., Masri, B., Malecaze, F., Knibiehler, B., and Audigier, Y. (2002) Expression of the murine msr/apj receptor and its ligand apelin is upregulated during formation of the retinal vessels. *Mech. Dev.* **110**, 183–186
46. Saint-Geniez, M., Argence, C.B., Knibiehler, B., and Audigier, Y. (2003) The msr/apj gene encoding the apelin receptor is an early and specific marker of the venous phenotype in the retinal vasculature. *Gene Expr. Patterns* **3**, 467–472
47. Jakobsson, L., Franco, C.A., Bentley, K., Collins, R.T., Ponsioen, B., Aspalter, I.M., Rosewell, I., Busse, M., Thurston, G., Medvinsky, A., Schuttle-merker, S., and Gerhardt, H. (2010) Endothelial cells dynamically compete for the tip cell position during angiogenic sprouting. *Nat. Cell Biol.* **12**, 943–953
48. Arima, S., Nishiyama, K., Ko, T., Arima, Y., Hakozaki, Y., Sugihara, K., Koseki, H., Uchijima, Y., Kurihara, Y., and Kurihara, H. (2011) Angiogenic morphogenesis driven by dynamic and heterogeneous collective endothelial cell movement. *Development* **138**, 4763–4776
49. del Toro, R., Prahst, C., Mathivet, T., Siegfried, G., Kaminker, J.S., Larrivee, B., Breant, C., Duarte, A., Takakura, N., Fukamizu, A., Penninger, J., and Eichmann, A. (2010) Identification and functional analysis of endothelial tip cell-enriched genes. *Blood* **116**, 4025–4033
50. Kasai, A., Shintani, N., Kato, H., Matsuda, S., Gomi, F., Haba, R., Hashimoto, H., Kakuda, M., Tano, Y., and Baba, A. (2008) Retardation of retinal vascular development in apelin-deficient mice. *Arterioscler. Thromb. Vasc. Biol.* **28**, 1717–1722
51. Sakimoto, S., Kidoya, H., Naito, H., Kamei, M., Sakaguchi, H., Goda, N., Fukamizu, A., Nishida, K., and Takakura, N. (2012) A role for endothelial cells in promoting the maturation of astrocytes through the apelin/APJ system in mice. *Development* **139**, 1327–1335
52. Seaman, S., Stevens, J., Yang, M.Y., Logsdon, D., Graff-Cherry, C., and St Croix, B. (2007) Genes that distinguish physiological and pathological angiogenesis. *Cancer Cell* **11**, 539–554
53. Wang, Z., Greeley, G.H. Jr, and Qiu, S. (2008) Immunohistochemical localization of apelin in human normal breast and breast carcinoma. *J. Mol. Histol.* **39**, 121–124
54. Kidoya, H., Kunii, N., Naito, H., Muramatsu, F., Okamoto, Y., Nakayama, T., and Takakura, N. (2011) The apelin/APJ system induces maturation of the tumor vasculature and improves the efficiency of immune therapy. *Oncogene*, doi: 10.1038/onc.2011.489
55. Berta, J., Kenessey, I., Dobos, J., Tovari, J., Klepetko, W., Jan Ankersmit, H., Hegedus, B., Renyi-Vamos, F., Varga, J., Lorincz, Z., Paku, S., Ostoros, G., Rozsas, A., Timar, J., and Dome, B. (2010) Apelin expression in human non-small cell lung cancer: role in angiogenesis and prognosis. *J. Thorac. Oncol.* **5**, 1120–1129
56. Sorli, S.C., Le Gonidec, S., Knibiehler, B., and Audigier, Y. (2007) Apelin is a potent activator of tumour neoangiogenesis. *Oncogene* **26**, 7692–7699
57. Jain, R.K. (2005) Normalization of tumor vasculature: an emerging concept in antiangiogenic therapy. *Science* **307**, 58–62
58. Dickson, P.V., Hamner, J.B., Sims, T.L., Fraga, C.H., Ng, C.Y., Rajasekeran, S., Hagedorn, N.L., McCarville, M.B., Stewart, C.F., and Davidoff, A.M. (2007) Bevacizumab-induced transient remodeling of the vasculature in neuroblastoma xenografts results in improved delivery and efficacy of systemically administered chemotherapy. *Clin. Cancer Res.* **13**, 3942–3950
59. Kunduzova, O., Alet, N., Delesque-Touchard, N., Millet, L., Castan-Laurell, I., Muller, C., Dray, C., Schaeffer, P., Herault, J.P., Savi, P., Bono, F., and Valet, P. (2008) Apelin/APJ signaling system: a potential link between adipose tissue and endothelial angiogenic processes. *FASEB J.* **22**, 4146–4153
60. Tiani, C., Garcia-Pras, E., Mejias, M., de Gottardi, A., Berzigotti, A., Bosch, J., and Fernandez, M. (2009) Apelin signaling modulates splanchnic angiogenesis and portosystemic collateral vessel formation in rats with portal hypertension. *J. Hepatol.* **50**, 296–305
61. Kidoya, H., Naito, H., and Takakura, N. (2010) Apelin induces enlarged and nonleaky blood vessels for functional recovery from ischemia. *Blood* **115**, 3166–3174
62. Sheikh, A.Y., Chun, H.J., Glassford, A.J., Kundu, R.K., Kutschka, I., Ardigo, D., Hendry, S.L., Wagner, R.A., Chen, M.M., Ali, Z.A., Yue, P., Huynh, D.T., Connolly, A.J., Pelletier, M.P., Tsao, P.S., Robbins, R.C., and Quertermous, T. (2008) In vivo genetic profiling and cellular localization of apelin reveals a hypoxia-sensitive, endothelial-centered pathway activated in ischemic heart failure. *Am. J. Physiol. Heart Circ. Physiol.* **294**, H88–H98
63. Sawane, M., Kidoya, H., Muramatsu, F., Takakura, N., and Kajiya, K Apelin attenuates UVB-induced edema and inflammation by promoting vessel function. *Am. J. Pathol* **179**, 2691–2697

Development 139, 1327-1335 (2012) doi:10.1242/dev.072330

A role for endothelial cells in promoting the maturation of astrocytes through the apelin/APJ system in mice

Susumu Sakimoto[1,2], Hiroyasu Kidoya[1], Hisamichi Naito[1], Motohiro Kamei[2], Hirokazu Sakaguchi[2], Nobuhito Goda[4], Akiyoshi Fukamizu[3], Kohji Nishida[2] and Nobuyuki Takakura[1,5,*]

SUMMARY

Interactions between astrocytes and endothelial cells (ECs) are crucial for retinal vascular formation. Astrocytes induce migration and proliferation of ECs via their production of vascular endothelial growth factor (VEGF) and, conversely, ECs induce maturation of astrocytes possibly by the secretion of leukemia inhibitory factor (LIF). Together with the maturation of astrocytes, this finalizes angiogenesis. Thus far, the mechanisms triggering LIF production in ECs are unclear. Here we show that apelin, a ligand for the endothelial receptor APJ, induces maturation of astrocytes mediated by the production of LIF from ECs. *APJ* (*Aplnr*)- and *Apln*-deficient mice show delayed angiogenesis; however, aberrant overgrowth of endothelial networks with immature astrocyte overgrowth was induced. When ECs were stimulated with apelin, LIF expression was upregulated and intraocular injection of LIF into *APJ*-deficient mice suppressed EC and astrocyte overgrowth. These data suggest an involvement of apelin/APJ in the maturation process of retinal angiogenesis.

KEY WORDS: Astrocytes, Endothelial cells, Apelin, Mouse

INTRODUCTION

The retina is composed of several cell types. Interactions between endothelial cells (ECs), astrocytes and neuronal cells is crucial for fine capillary network formation by ECs. Before the onset of interactions between ECs and astrocytes in the retina of postnatal mice, astrocytes invade from the optic nerve head via the axons of retinal ganglion cells. Controlling this association between different cell components, platelet-derived growth factor A (PDGFA) from retinal ganglion cells promotes growth of immature astrocytes expressing PDGF receptor α (PDGFRα). This results in astrocyte network formation (Fruttiger et al., 1996). Subsequently, ECs from the optic nerve head invade and migrate over the network-forming astrocytes as a template. A crucial role of vascular endothelial growth factor (VEGF), produced by astrocytes, in guiding endothelial tip cells in the vascular branch and in the proliferation of endothelial stalk cells behind the tip cells has been reported (Gerhardt et al., 2003).

In the course of retinal angiogenesis, astrocytes act as proangiogenic accessory cells, as described above; however, upon becoming overlaid with ECs, it has been suggested that their proangiogenic activity ceases and they instead stabilize newly developed blood vessels (West et al., 2005; Kubota et al., 2008). Anatomical analysis has revealed that astrocytes expressing low levels of glial fibrillary acidic protein (GFAP) firstly invade the retina, gradually express higher levels of GFAP, and become quiescent (Chu et al., 2001; Gariano, 2003). Therefore, it has been suggested that ECs might change astrocyte characteristics (Zhang and Stone, 1997), with several lines of evidence suggesting that leukemia inhibitory factor (LIF) derived from ECs is a direct maturation factor for immature astrocytes in vitro (Mi et al., 2001) and in vivo (Kubota et al., 2008). However, the mechanism responsible for controlling LIF production by ECs for maturation of astrocytes has not been elucidated.

During the process of angiogenesis, maturation of blood vessels is induced by angiopoietin 1 (ANG1; also known as ANGPT1), a ligand for endothelial receptor tyrosine kinase TIE2 (also known as TEK), produced by mural cells, which directly adhere to ECs. This results in structural stabilization of the blood vessels (Sato et al., 1995; Suri et al., 1996; Augustin et al., 2009). Apelin is a ligand for the G protein-coupled receptor APJ expressed on ECs. We previously reported that activation of TIE2 promotes apelin production from ECs and that ANG1/TIE2-mediated maturation of blood vessels, such as their enlargement and non-leaky blood vessel formation, is partly dependent on APJ activation by apelin ligation (Kidoya et al., 2008; Kidoya et al., 2010). Recently, involvement of the apelin/APJ system in retinal angiogenesis has been reported (Kasai et al., 2008; del Toro et al., 2010) in which delayed angiogenesis and reduced proliferation of stalk cells was observed in gene ablation analysis of apelin (*Apln*) and apelin receptor (*APJ*; *Aplnr* – Mouse Genome Informatics) (Kasai et al., 2008; del Toro et al., 2010; Kidoya et al., 2010). In contrast to the constitutive expression of TIE2, as well as of VEGF receptor 2 (VEGFR2; also known as FLK1 and KDR), APJ expression in ECs is transient. From the onset of retinal angiogenesis, most network-forming ECs express APJ until postnatal day (P) 7; however, after reaching the marginal zone of the retina, ECs stop expressing APJ at P12, except for the larger veins (Saint-Geniez et al., 2003). Taken together, these findings imply that apelin/APJ acts as a maturation factor for newly developed blood vessels, in addition to its proangiogenic function.

During retinal angiogenesis, it is suggested that ECs and astrocytes mature simultaneously in a mutually dependent manner. However, whether maturation arrest of blood vessels affects

[1]Department of Signal Transduction, Research Institute for Microbial Diseases, Osaka University, 3-1 Yamada-oka, Suita, Osaka 565-0871, Japan. [2]Department of Ophthalmology, Osaka University Graduate School of Medicine, Suita, Osaka 565-0871, Japan. [3]Center for Tsukuba Advanced Research Alliance, Institute of Applied Biochemistry, University of Tsukuba, Ibaraki 305-8577, Japan. [4]Department of Life Science and Medical Bio-Science, School of Advanced Science and Engineering, Waseda University, 2-2 Wakamatsu-cho, Shinjuku-ku, Tokyo 162-8480, Japan. [5]JST, CREST, K's Gobancho, 7 Gobancho, Chiyoda-ku, Tokyo 102-0076, Japan.

*Author for correspondence (ntakaku@biken.osaka-u.ac.jp)

Accepted 15 January 2012

astrocyte maturation is not yet clear. Because apelin/APJ is mainly involved in the maturation of blood vessels, we used mice with *Apln* as well as *APJ* mutations to ask whether the maturation of astrocytes is affected by a deficiency of apelin or APJ. Moreover, we investigated how astrocyte maturation conversely affects the growth of ECs in order to understand mutual EC/astrocyte regulation.

MATERIALS AND METHODS

Mice

All experiments were carried out under the guidelines of the Osaka University Committee for Animal Research. C57BL/6 (Japan SLC, Shizuoka, Japan), *APJ* knockout (KO) (Ishida et al., 2004) and *Apln* KO (Kidoya et al., 2008) mice were used in these studies. Animals were housed in environmentally controlled rooms of the animal experimentation facility at Osaka University.

Quantitative reverse transcription real-time PCR (qRT-PCR)

Total RNA was extracted from cells and tissues using the RNeasy Plus Mini Kit (Qiagen) and transcribed into cDNA using the ExScript RT Reagent Kit (Takara) according to the manufacturers' protocols. Real-time PCR analysis was performed using Platinum SYBR Green qPCR SuperMix-UDG (Invitrogen) and an Mx3000P QPCR System (Stratagene). The baseline and threshold were adjusted according to the manufacturer's instructions. PCR was performed on cDNA using the primers listed in supplementary material Table S1. The level of expression of the target gene was normalized to that of *Gapdh* in each sample.

Tissue immunostaining and in situ hybridization (ISH)

Tissue preparation and staining were as previously reported (Takakura et al., 2000). Enucleated eyes were fixed in 4% paraformaldehyde. Antibodies for staining were anti-PECAM1 (BD Biosciences, 1:100; or Chemicon International, 1:100), anti-GFAP (Sigma-Aldrich, 1:100), anti-PDGFRα (eBioscience, 1:100), anti-desmin (DAKO, 1:100), anti-PAX2 (Covance, 1:100), anti-KI67 (DAKO, 1:100), anti-neurofilament (American Research Products, 1:100), anti-type IV collagen (Cosmo Bio, 1:100), anti-HIF1α (1:100) (Kurihara et al., 2010), anti-apelin (1:100) (Kidoya et al., 2008) and anti-APJ (1:100) (Kidoya et al., 2008). The secondary antibodies used were Alexa Fluor 488/546/647-conjugated IgGs (Invitrogen, 1:200) or FITC/Cy5-conjugated IgGs (Jackson ImmunoResearch Laboratories, 1:200).

For whole-mount ISH, retinas were briefly digested with proteinase K and hybridized with digoxigenin-labeled antisense RNA probes.

For determination of hypoxic tissue, mice were injected intraperitoneally with 60 mg/kg body weight Hypoxyprobe-1 (pimonidazole hydrochloride) (Natural Pharmacia International) before harvesting retinas for tissue processing and staining according to the manufacturer's instructions. Six animals per group were analyzed. A total of eight straight lines were drawn in each retina: four from the optic nerve to the vascular front representing a vascularized area; and four from the vascular front to the peripheral retina as an avascular area. Samples were visualized using conventional microscopy (with a DM5500B equipped with HCX PL FLVOTAR 5/0.15 and HCX PL FLVOTAR 0/0.15 dry objective lenses, Leica) or confocal microscopy (TCS/SP5 equipped with HC PLAN APO 2/0.70 and HCXPL APO 4/1.25-0.75 oil objective lenses, Leica) at room temperature. Images were acquired with a DFC 500 digital camera (Leica) and processed with the Leica application suite and Adobe Photoshop CS3 software. All images shown are representative of three to six independent experiments.

Retina quantification

Complete high-resolution three-dimensional (3D) rendering of whole-mount retinas was achieved using the confocal microscope described above. The cells of interest ($PAX2^+$ astrocytes, $PAX2^+$ $KI67^+$ astrocytes and $HIF1\alpha^+$ cells) were manually scored in six random 350×350 μm or 250×250 μm ($HIF1\alpha^+$ cells) fields of view (FOV) per retina photographed at 40× or 63× magnification using the software of the Leica application suite. To determine cell number and measure the capillary density of the retinas, six animals per group were analyzed. After conversion to 8-bit grayscale using ImageJ software, the capillary density in the vascularized area was quantified from the pixels. The vascularized areas were defined as the region near the vascular front without the regions from the very tips to the first vascular loop. The avascular areas were defined as the regions ~500 μm ahead of the vascular front. $HIF1\alpha^+$ cells were counted in different areas.

Flow cytometry analysis

Retinas of at least five WT and *APJ* KO mouse neonates were incubated for 30 minutes at 37°C in DMEM containing 1% collagenase (Wako, Osaka, Japan) before cells were dissociated by gentle trituration. Cells were pretreated with Fc-Blocker (BD Biosciences Pharmingen) and stained with FITC-conjugated anti-CD140a (PDGFRα) monoclonal antibody and phycoerythrin-conjugated anti-CD31 monoclonal antibody (BD Biosciences Pharmingen). Procedures for cell preparation and staining were as previously reported (Kidoya et al., 2008). The stained cells were analyzed and sorted using a FACSAria flow cytometer (BD) with FlowJo (TreeStar) or CellQuest (BD) software. Dead cells were excluded from the analyses using the 2D profile of forward versus side scatter. Using these negative and positive control tubes, we set fluorescence voltages and the compensation matrix according to the instructions of the manufacturer. We applied these setting parameters to all samples analyzed.

Intraocular injection

Sterile PBS with or without 1 mg/ml apelin (Bachem), 0.5 mg/ml LIF (ESGRO, Chemicon) or 1 mg/ml sFLT1 was injected into the vitreous humor of P3 mice using a sterile injection capillary with an automatic microinjector (FemtoJet, Eppendorf). Mice were sacrificed 48 hours later and the retinas isolated for cell purification or immunohistochemistry.

Cell culture

The mouse microvascular endothelial cell line bEnd.3 or HUVECs were cultured in six-well plates for 12 hours in DMEM or Humedia EG2 (Kurabo, Osaka, Japan), respectively. Cells were then incubated in medium supplemented with 1% fetal bovine serum (FBS). After 6 hours of serum deprivation, cells were stimulated with basal medium containing 20 ng/ml VEGFA 165 (PeproTech) for 18 hours and subsequently incubated with 50 or 500 ng/ml apelin. Culturing of retinal cells was performed as described previously (West et al., 2005). P1 WT retinas were dissected as indicated above, redissociated in DMEM containing 10% FBS and then plated on poly-D-lysine-coated coverslips in 24-well plates at 1.5×10^6 cells/well and incubated at 37°C, 5% CO_2 for 24 hours. Retinal cells were incubated for 24 hours with supernatant of bEnd.3 cells that had been treated with apelin for 24 hours.

Statistical analysis

Data are presented as mean±s.d. for the in vitro studies and mean±s.e. for in vivo studies. For statistical analysis, the Statcel 2 software package (OMS) was used with analysis of variance performed on all data followed by Tukey-Kramer multiple comparison testing. When only two groups were compared, a two-sided Student's *t*-test was used. $P<0.05$ was considered statistically significant.

RESULTS

Dense astrocyte network formation is induced in APJ-deficient mice

Because it has been reported that *APJ* mutant mice show retarded endothelial network formation in the retina (del Toro et al., 2010), we first investigated the development of, and network formation by, astrocytes from P0 to P7 (Fig. 1A). Using anti-PDGFRα antibody in immunohistochemistry (IHC) to identify these cells, we found that astrocyte network formation was similar in wild-type (WT) and *APJ* KO mice at P1; however, a dense network appeared in *APJ* KO mice at P5 and continued at least until P7. $PDGFR\alpha^+$ astrocytes were also analyzed by flow cytometry and their number calculated as a proportion of the total number of retinal cells at P5. A significantly greater proportion of astrocytes was found to be present in *APJ* KO

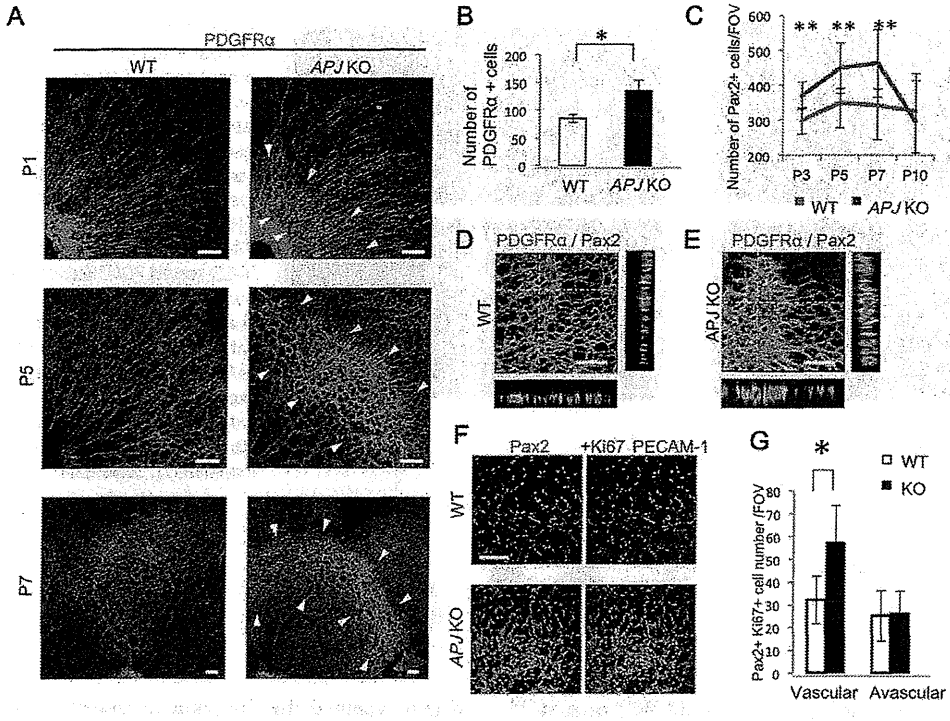

Fig. 1. *APJ* KO mice show irregular remodeling and proliferation of retinal astrocytes. (**A**) Immunohistochemistry (IHC) for PDGFRα (green) in the P1, P5 and P7 developing retina of wild-type (WT) or *APJ* KO mice. Note the dense astrocyte network (surrounded by arrowheads) in *APJ* KO mice. (**B**) Quantitative evaluation of the number of PDGFRα$^+$ cells per 5×10^4 cells analyzed by FACS. Dissociated retinal cells from P5 WT or *APJ* KO mice were used (n=4, *P<0.05). (**C**) Transition of the number of astrocytes identified as PAX2$^+$ nuclei in vascularized areas. Data are the mean of six random fields of view (FOV) in the vascularized area per retina (n=6, **P<0.01). (**D,E**) Confocal microscopy images of PDGFRα$^+$ (green) and PAX2$^+$ (red) astrocytes in WT (D) and *APJ* KO (E) P5 retinas. z-stack images show two-layered astrocytes in *APJ* KO retina. (**F**) Proliferation status of astrocytes in P5 retinas from WT and *APJ* KO mice. Retinas were stained with antibodies against PAX2 (green), KI67 (magenta) and PECAM1 (blue). Note the marked proliferation of PAX2$^+$ KI67$^+$ astrocytes (white or light blue) in vascular areas of *APJ* KO mice. (**G**) Quantification of PAX2$^+$ KI67$^+$ astrocytes in the vascularized or non-vascularized retinal areas. Six random FOV were examined per retina (n=6,*P<0.05). Error bars indicate s.d. Scale bars: 100 μm.

than WT mice (Fig. 1B). We next calculated the number of astrocytes expressing PAX2, a nuclear transcription factor present in all cells of the astrocyte lineage (Fig. 1C-E). Although the number of PAX2$^+$ astrocytes in *APJ* KO mice was higher than in WT mice from P3 to P7, it gradually decreased to WT levels, suggesting negative-feedback regulation (Fig. 1C). z-stack images suggested that a thicker retinal astrocyte layer was induced in *APJ* KO than in WT mice owing to the generation of two layers of astrocytes at P5 (Fig. 1D,E). Next, we stained the retina for the EC marker PECAM1 (CD31) and with anti-PAX2 antibody, as well as for the cell proliferation marker (KI67). High-density areas of PAX2$^+$ KI67$^+$ proliferating astrocytes were present in vascular but not avascular areas (Fig. 1F,G), suggesting that astrocyte proliferation is associated with ECs.

Next we assessed the degree of astrocyte maturation in *APJ* KO mice. In WT mice, astrocytes that are initially weakly GFAP positive start to express a high level of GFAP at P5 (Fig. 2A-C). The strongly GFAP-positive astrocytes present from the optic nerve head up to the beginning of the dense astrocyte sheet area did not differ substantially between *APJ* KO and WT mice. However, within the dense astrocyte sheet there were fewer strongly GFAP-positive astrocytes in the *APJ* KO mice (Fig. 2A,D,E). Consistent with this, levels of *Gfap* mRNA were reduced in *APJ* KO mice at all periods examined (Fig. 2F). Comparing other astrocyte differentiation markers in *APJ* KO and WT mice revealed similar levels of expression for the lineage markers vimentin (*Vim*) and *Pax2* but a significant reduction in the mature astrocyte markers *S100b* and *Gfap* in the knockouts (Fig. 2G). These data suggest that APJ deficiency does not affect the development of astrocytes but influences their maturation.

APJ deficiency indirectly induces dense endothelial sheets via overgrowth of immature astrocytes

It has been reported that both *APJ* KO and *Apln* KO mice show delayed retinal angiogenesis (Kasai et al., 2008; del Toro et al., 2010). However, as we found aberrant overgrowth of immature astrocytes in *APJ* KO mice, we hypothesized that abnormal overgrowth during blood vessel formation should also be induced in *APJ* KO mice indirectly owing to the defect of APJ in ECs, as weakly GFAP-positive astrocytes possess proangiogenic properties. Although retinal vessel outgrowth from the optic nerve head was indeed impaired in *APJ* KO mice (supplementary material Fig. S1) as previously reported (del Toro et al., 2010), a dense endothelial network-forming area was frequently observed at the migrating front of the retinal vasculature after P5 (Fig. 3A-C).

Consistent with hyperproliferation of ECs in *APJ* KO mice, the retinas of these mice were found by in situ hybridization (ISH) to express more *Vegfa* mRNA in the peripheral region of

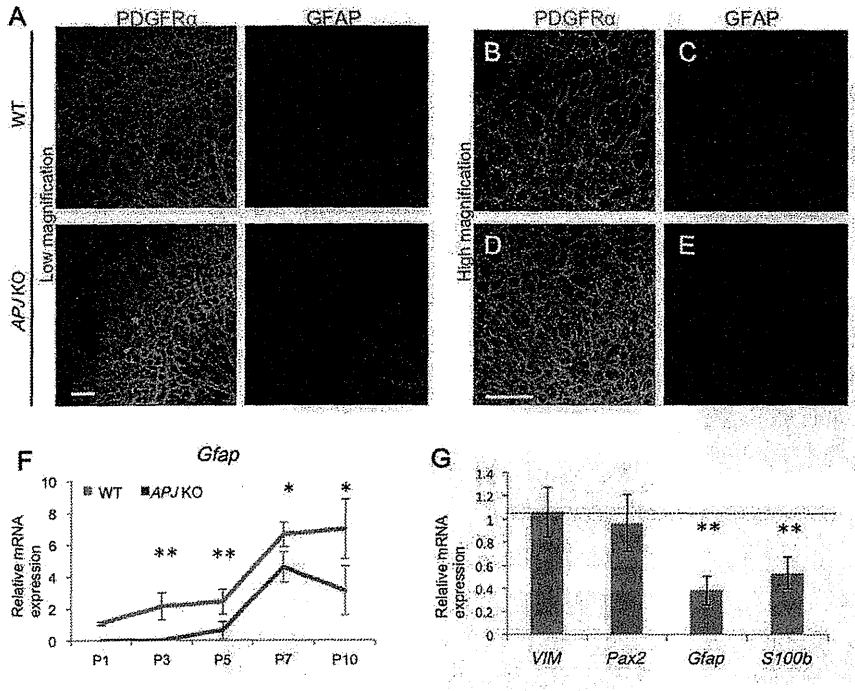

Fig. 2. Suppression of astrocyte maturation in *APJ* KO developing retina. (**A**) Retinal astrocytes stained for PDGFRα (green) and GFAP (red) in P5 WT and *APJ* KO mice. (**B-E**) High-magnification views of retinal astrocytes around the migrating front of the vascular network area as shown in Fig. 1F. Note the weak positivity for GFAP in overgrown astrocytes in *APJ* KO mice. (**F**) Quantitative RT-PCR (qPCR) analysis of *Gfap* expression using isolated RNA from FACS-sorted PDGFRα$^+$ cells at various retinal stages (n=3, *P<0.05, **P<0.01). (**G**) qPCR analysis of retinal astrocyte marker expression with RNA isolated from sorted PDGFRα$^+$ cells of P5 retina. Data represent relative mRNA expression from *APJ* KO mice as compared with WT mice set as unity (n=3, **P<0.01). Dotted line indicates level of WT. Error bars indicate s.d. Scale bars: 100 μm.

the endothelial network-forming area than did WT mice at P5 (Fig. 3D). Moreover, comparing sorted retinal PDGFRα$^+$ astrocytes revealed greater *Vegfa* mRNA expression in *APJ* KO than in WT mice (Fig. 3E). VEGF expression is known to be regulated by hypoxia via hypoxia inducible factor 1α (HIF1α). It has been reported that suppression of retinal vascular growth by VEGF-Trap injections primarily leads to VEGF upregulation, GFAP downregulation, and dense network formation in retinal astrocytes (Uemura et al., 2006). Moreover, West et al. have clearly demonstrated that hypoxia inhibits the maturation of astrocytes, resulting in VEGF upregulation, using models for retinopathy of prematurity (West et al., 2005). Currently, it is widely accepted that hypoxia is crucial for the regulation of astrocyte maturation. Therefore, it is possible that the hyperproliferation of ECs observed in *APJ* KO mice is caused by hypoxia induced by impaired vessel outgrowth. Indeed, compared with WT mice, slightly stronger Hypoxyprobe-1 signals were observed in the avascular area of the vascular front (asterisks in Fig. 4A,B) and the hypovascular areas in the middle of the vascular network (the areas enclosed by the dashed lines in Fig. 4A) in *APJ* KO mice. Although the levels of *Hif1a* mRNA were not significantly different in the whole retinas of WT and *APJ* KO mice (supplementary material Fig. S3), nuclear translocation of HIF1α, indicating its state of activation, was

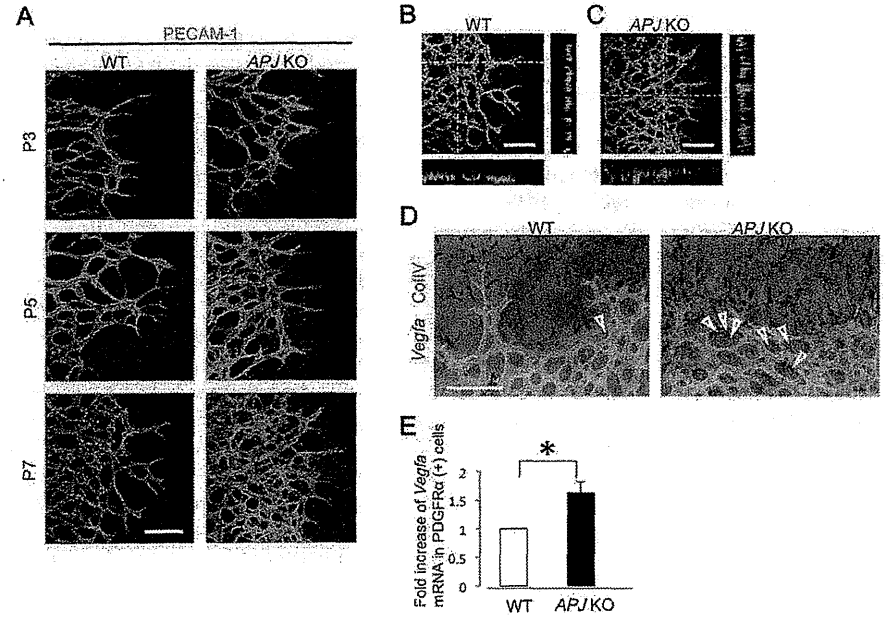

Fig. 3. Aberrant overgrowth of ECs in *APJ* KO mice. (**A**) Whole-mount anti-PECAM1 immunostaining of the developing retina around the vascular front of P3, P5 and P7 WT and *APJ* KO mice. (**B,C**) Confocal microscopy images of PECAM1$^+$ ECs in P7 WT (B) and *APJ* KO (C) mouse retinas. *z*-stack images show a denser EC layer in *APJ* KO than in WT retina. (**D**) In situ hybridization (ISH) for *Vegfa* combined with IHC for collagen IV in the vascular front. Note the increase of *Vegfa* mRNA in *APJ* KO retina. Arrowheads indicate upregulation of *Vegfa* mRNA even in the vascular area. (**E**) qPCR analysis of *Vegfa* mRNA expression in retinal PDGFRα$^+$ astrocytes from P5 retinas of WT and *APJ* KO mice (n=3, *P<0.05). Error bars indicate s.d. Scale bars: 100 μm.

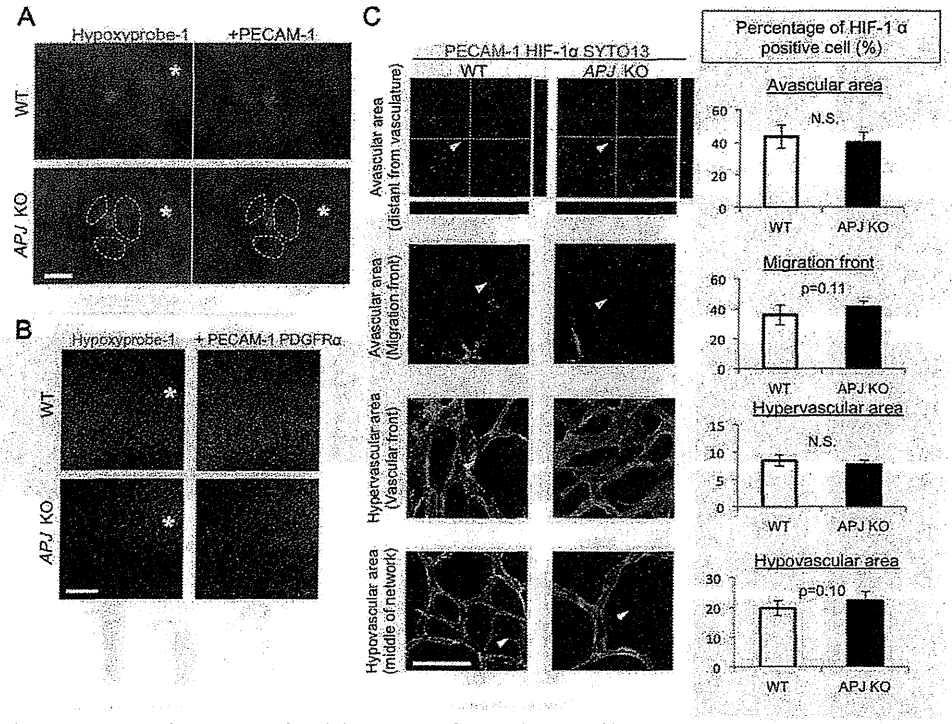

Fig. 4. Evaluation of hypoxic status in *APJ* KO mice. (**A**) Low-magnification images of hypoxic status in *APJ* KO mouse retina. Detection of PECAM1 (red) and Hypoxyprobe-1 (green) in P5 WT and *APJ* KO retinas. Asterisks indicate avascular areas of the vascular front and the areas demarcated by dashed lines indicate the hypovascular areas in the middle of the vascular network. (**B**) Higher magnification images of hypoxic status showing PECAM1 (red), PDGFRα (blue) and Hypoxyprobe-1 (green) in P5 WT and *APJ* KO retinas. (**C**) Nuclear translocation of HIF1α protein in *APJ* KO mice. Retinas of WT and *APJ* KO mice were dissected at P5 and whole-mount immunostaining was performed using anti-PECAM1 (green) and anti-HIF1α (red) antibodies and analyzed in different areas. Arrowheads indicate nuclear positivity for HIF1α. *z*-stack image showing localization of HIF1α in nuclei stained with SYTO13 (blue). (Right) Percentages of nuclear HIF1α$^+$ cells in the areas described were quantitatively evaluated. Four random FOV in the vascularized area were examined per retina (n=6). N.S., not significant. Error bars indicate s.d. Scale bars: 500 μm in A; 100 μm in B; 50 μm in C.

slightly enhanced in areas where more intense Hypoxyprobe-1 signals were observed in the *APJ* KO mice (Fig. 4C). However, the difference in HIFα nuclear translocation in WT and *APJ* KO mice was not statistically significant.

These data suggest that the VEGFA overexpression observed in astrocytes from *APJ* KO mice and the partial dense vascular network formation are dependent on hypoxia as a primary effect of APJ deficiency. However, compared with other models using VEGF-Trap (Uemura et al., 2006) or retinopathy of prematurity (West et al., 2005), in which blood vessel formation in the retina is completely abolished and strong hypoxia is induced, the degree of vascular defects and hypoxia observed here in *APJ* KO mice was not severe. Therefore, we consider that not only hypoxia but also other mechanisms underlie the maturation of astrocytes affected by APJ.

It is possible that APJ is expressed on astrocytes and that this, rather than its absence from ECs, affects the growth of immature astrocytes directly. However, we were unable to detect APJ expression on PDGFRα$^+$ astrocytes, whereas it was present on ECs (supplementary material Fig. S2). Moreover, we assessed whether the overgrowth of astrocytes is affected by aberrant growth of retinal ganglion cells. As shown in Fig. 5A, radially migrated well-organized retinal ganglion cells were present in *APJ* KO mice to the same extent as in WT mice. Expression of *Pdgfa* mRNA in retinal tissue was not increased in *APJ* KO mice relative to WT mice (Fig. 5B).

Next, we tested whether moderate, but not severely, delayed angiogenesis in the retina, as observed in *APJ* KO mice, affects astrocyte proliferation in WT mice by neutralizing VEGF using injections of soluble (s) FLT1 (VEGFR1). We started to neutralize VEGF from P3 and assessed its effects on vascular formation at P5, as severe vascular defects were induced when VEGF was neutralized from P0, as previously reported (Uemura et al., 2006). As shown in Fig. 5C, treatment with sFLT1 according to this schedule retarded the outgrowth of blood vessels to a similar extent to that observed in *APJ* KO mice. Although a partial dense astrocyte sheet was observed (Fig. 5C, arrow), *z*-stack images suggested that the thickness of the astrocyte layer was almost the same in PBS-treated or sFLT1-treated mice (Fig. 5D). Furthermore, increases in the total number and proliferation of astrocytes were not observed (Fig. 5E-H). These data suggest that molecular cues that are absent owing to the lack of APJ in ECs affect overgrowth by immature astrocytes.

Exogenous apelin induces the expression of GFAP in retinal astrocytes

Based on this result that a lack of APJ on ECs affects the outgrowth of immature astrocytes, we next examined whether apelin is involved in astrocyte differentiation and proliferation in vivo. Immunohistochemical analysis revealed that GFAP expression on astrocytes at P5 was enhanced following intraocular injection of apelin into WT mice at P3 (Fig. 6A). We confirmed upregulation

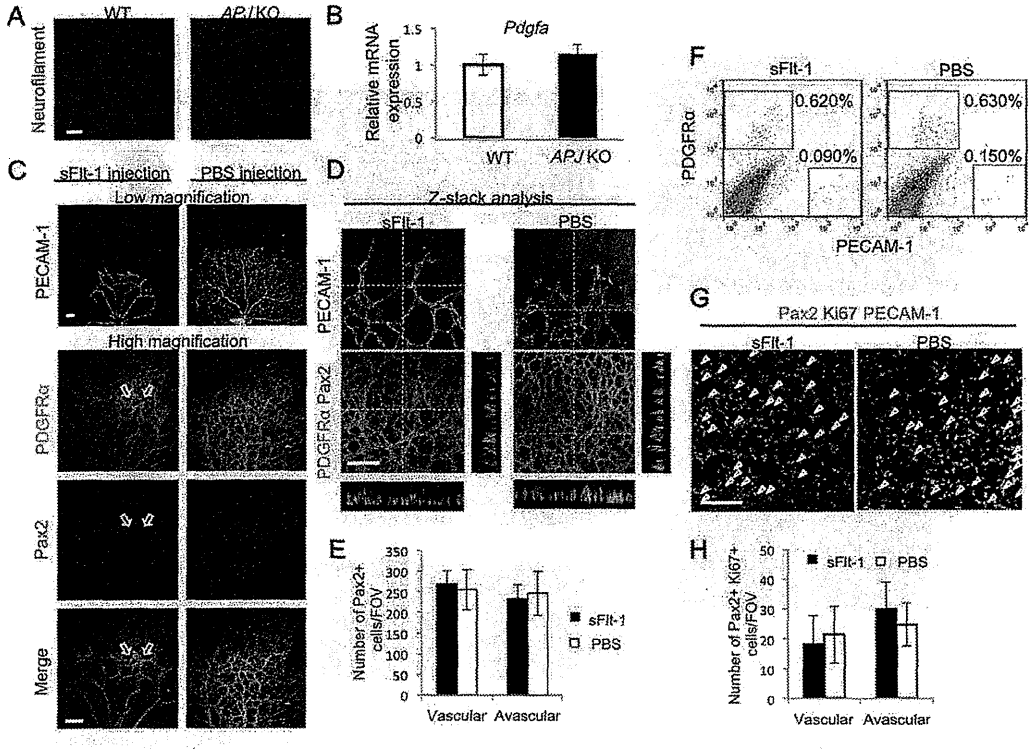

Fig. 5. Evaluation of neuronal cell development in the absence of APJ and its effects on proliferation of astrocytes mediated by retardation of vascular development. (**A**) The morphology of retinal ganglion cells in P3 WT and *APJ* KO mouse retinas. Retinas were stained with anti-neurofilament antibody. (**B**) qPCR analysis of *Pdgfa* mRNA expression in P5 WT and *APJ* KO retinas. (**C-G**) Effect of vascular retardation on astrocyte development in the retina assessed by intraocular injection of soluble (s) FLT1 or PBS (control). (C) Retinas were stained with antibodies against PDGFRα (green), PAX2 (red) and PECAM1 (white) at P5, 48 hours after treatment with sFLT1 or PBS. Although sFLT1 retarded vascular outgrowth, this degree of vascular defectiveness did not induce substantially abnormal networks of astrocytes at the vascular front with the exception of slight dense astrocyte network formation (arrows in C). (D) *z*-stack imaging showing no differences in the thickness of the glial cell layer or in the number of PAX2$^+$ cells between PBS- and sFLT1-treated mice. (E) Quantification of PAX2$^+$ astrocytes in the vascular and avascular areas. (F) Flow cytometry analysis of P5 retina from PBS- and sFLT1-treated mice (n=8). The number of PECAM1$^+$ cells decreased with sFLT1 treatment but the number of PDGFRα$^+$ cells did not change. (G) Proliferation status of astrocytes in P5 retinas from PBS- and sFLT1-treated mice. Retinas were stained with antibodies against PAX2 (green), KI67 (magenta) and PECAM1 (blue). Arrowheads indicate PAX2$^+$ KI67$^+$ astrocytes in vascular areas of P5 retinas from PBS- and sFLT1-treated mice. (**H**) Quantification of PAX2$^+$ KI67$^+$ astrocytes in the vascularized and non-vascularized retinal areas. Four random FOV per retina were examined (n=5). Error bars indicate s.d. Scale bars: 100 μm.

of *Gfap* mRNA in sorted PDGFRα$^+$ astrocytes from retinal tissues (Fig. 6B). Contrary to expectations, however, additional apelin in the WT retina did not alter blood vessel formation (Fig. 6A,C).

Next, we assessed whether apelin affected overgrowth by astrocytes in *Apln* KO mice. As in *APJ* KO mice, hyperproliferation of PDGFRα$^+$ PAX2$^+$ astrocytes was observed in *Apln* KO mice at P5 (Fig. 6D). Such astrocytes were weakly positive for GFAP (data not shown). Similar to the experiment shown in Fig. 6A, *Apln* KO mice at P3 were given intraocular injections of apelin and retinal gliogenesis was observed at P5. This demonstrated that apelin prevented the hyperproliferation of astrocytes that would otherwise result from the lack of apelin (Fig. 6D,E). Moreover, the capillary density in the migrating front of the vascular network was decreased in *Apln* KO mice injected intraocularly with apelin (Fig. 6D,F).

Because we failed to detect APJ expression in astrocytes, it is possible that ECs produce maturation factors for astrocytes when they are stimulated by apelin. We added supernatants from 24-hour apelin-stimulated cultures of cells of the bEnd3 EC line derived from mouse brain to primary cultures of retinal cells from WT mice at P1 (Fig. 7A). We did not detect a direct effect of apelin on the induction of GFAP expression by astrocytes, but these culture supernatants enhanced its expression in retinal cells. Candidate factors for inducing GFAP positivity in astrocytes are LIF and ciliary neurotrophic factor (CNTF), which are both members of the IL6 family (Kishimoto et al., 1995). We investigated the expression of IL6 family cytokines in PECAM1$^+$ ECs directly sorted from the retina of *APJ* KO mice or WT mice at P5. We could not detect IL6, oncostatin M, cardiotrophin 1 or IL11 in ECs from WT or *APJ* KO mice, and CNTF expression was similar in ECs from both sources. By contrast, LIF expression was markedly lower in *APJ* KO than in WT mice (Fig. 7B). Transcription of *LIF* was upregulated transiently upon stimulation of human umbilical vein ECs (HUVECs) with apelin (Fig. 7C). These data suggest that stimulation of ECs by apelin induces production of LIF in an APJ-dependent manner, which then influences astrocyte maturation.

Overgrowth of immature astrocytes resulting from a lack of APJ in ECs is abrogated by LIF injection

On the basis of the above results, we suggest that a lack of apelin/APJ system activity in ECs induces overgrowth of immature astrocytes followed by inhibition of their maturation,

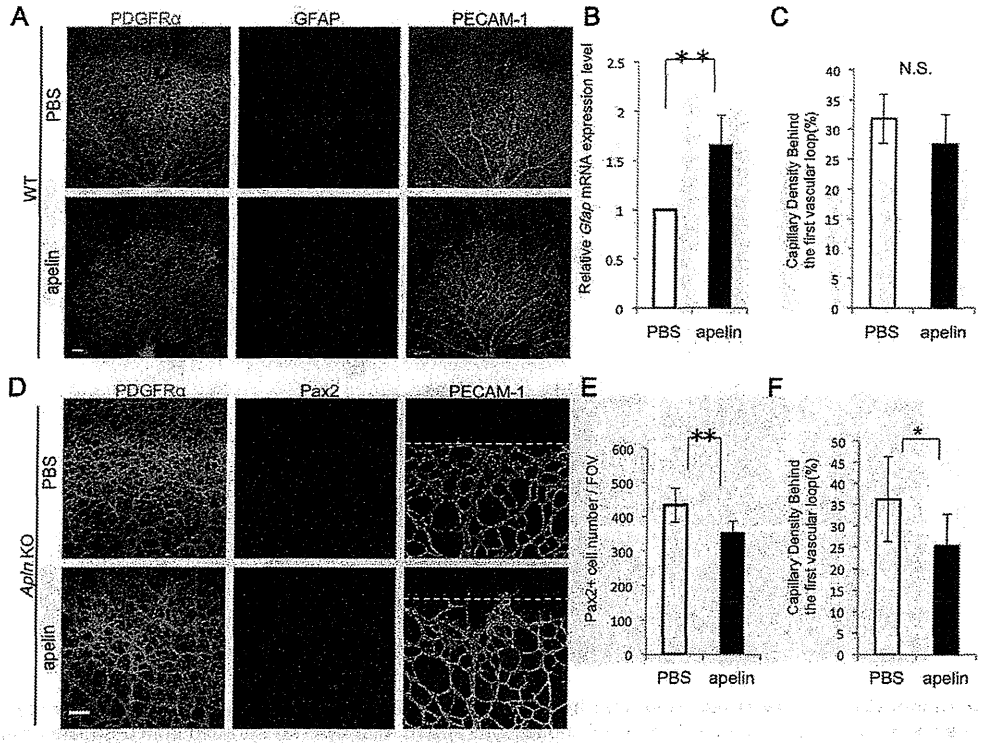

Fig. 6. Exogenous apelin-13 induces the expression of GFAP in retinal astrocytes. (**A-C**) Effect of apelin-13 in WT mouse retina. (A) Retinas were stained with antibodies against PDGFRα, GFAP and PECAM1 at P5, 48 hours after intraocular injection with PBS or apelin-13. (B) qPCR analysis of *Gfap* using mRNA from FACS-sorted PDGFRα$^+$ cells of P5 retina (**P<0.01). (C) Capillary density behind the first vascular loop after injection with apelin in WT mouse retina (n=6). N.S., not significant. (**D-F**) Rescue of aberrant overgrowth of astrocytes observed in *Apln* KO mice by intraocular injection of apelin-13. (D) Retinas were immunostained for PDGFRα, PAX2 and PECAM1 at P5, 48 hours after intraocular injection of PBS or apelin-13. (E) Quantitative evaluation of PAX2$^+$ astrocytes. Six random FOV in the retina were examined (n=6, **P<0.01). (F) Apelin reduces the capillary density from the vascular front in *Apln* KO mice (n=6, *P<0.05). The yellow dashed lines (D) demarcate the area (the first vascular loop) for which vascular density was calculated (C,F). Error bars indicate s.d. Scale bars: 100 μm.

resulting in aberrant EC network formation. Because LIF is upregulated upon stimulation of APJ by apelin in ECs, and because LIF is widely accepted as a maturation factor for astrocytes (Bonni et al., 1997; Mi et al., 2001), we injected LIF into *APJ* KO mice to assess whether maturation of astrocytes inhibits overgrowth of ECs as well as astrocytes. Intraocular injection of LIF into *APJ* KO mice at P3 resulted in a reduction of the number of PDGFRα$^+$ astrocytes and improved the formation of dense sheets of astrocytes (Fig. 7D). Moreover, weakly GFAP-positive astrocytes became strong GFAP expressors. Furthermore, staining with anti-PECAM1 antibody indicated that aberrant overgrowth of ECs was not induced. Quantitative evaluation of the number of astrocytes (confirmed by PAX2 staining) revealed that the hyperproliferation observed in the vascular area was reduced, but that LIF injection did not influence the number of astrocytes in the avascular area where no overgrowth had previously been observed (Fig. 7E). It is accepted that immature weakly GFAP-positive astrocytes induce proliferation of ECs but that this is gradually reduced as their level of GFAP expression increases (Kubota et al., 2008; West et al., 2005). This was suggested to be caused by the expression of VEGF in immature astrocytes. We assessed *Vegf* mRNA expression in retinal PDGFRα$^+$ astrocytes from *APJ* KO mice at P5. We found that LIF injection attenuated *Vegf* transcription (Fig. 7F), suggesting induction of astrocyte maturation.

DISCUSSION

Using a model of retinal angiogenesis, we have identified a possible mechanism by which maturation of astrocytes is induced as angiogenesis is finalized and newly developed blood vessels are consolidated. This entails apelin stimulation of APJ in ECs and subsequent LIF production, which induces maturation of weakly to strongly GFAP-positive astrocytes, which then enter quiescence. Because weakly GFAP-positive astrocytes act as proangiogenic accessory cells for ECs by producing VEGF and proliferate vigorously in response to PDGFA produced by ganglion cells, when LIF production is decreased due to the lack of apelin or APJ, the resulting aberrant overgrowth of immature astrocytes induces hyperproliferation of ECs. We propose that apelin/APJ activation in ECs is a trigger for finalization of blood vessel formation, indirectly mediated by the induction of astrocyte maturation.

We previously reported that although APJ is not expressed on ECs in the steady state after birth, in adulthood ischemia induces transient APJ expression in ECs mediated by stimulation with VEGF (Kidoya et al., 2008). In the retina, from the onset of retinal angiogenesis in newborn mice, network-forming ECs also transiently express APJ, which is downregulated after the establishment of the retinal endothelial network at P12 (Saint-Geniez et al., 2003). It has been reported using ISH that apelin is produced in tip cells, which might then induce proliferation of the stalk cells migrating behind them (del Toro et al., 2010). Apelin is secreted as peptides of 13 or 36 amino

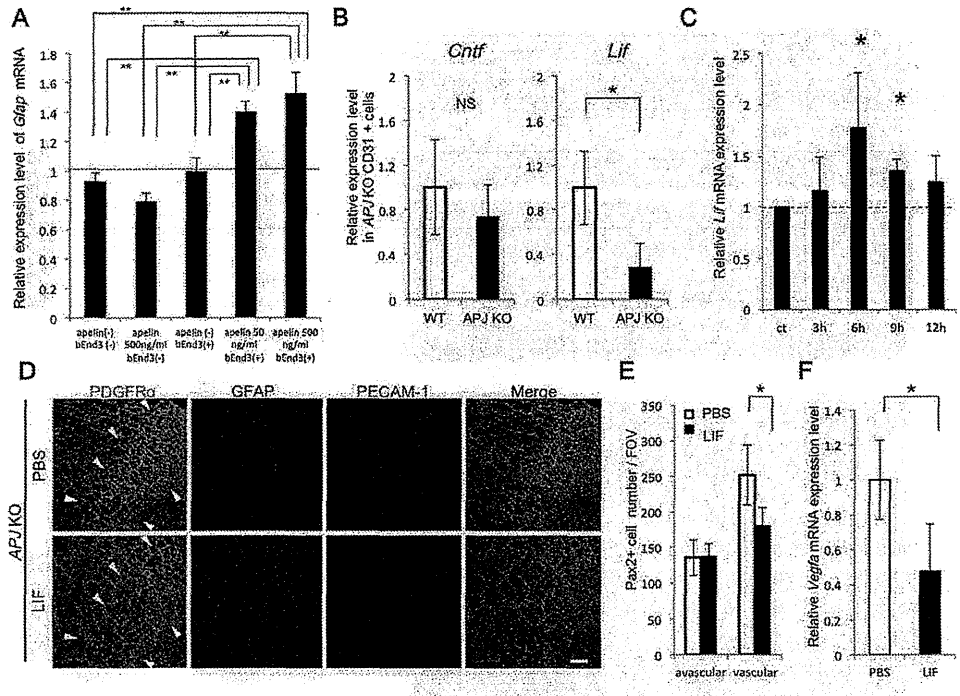

Fig. 7. Overgrowth of immature astrocytes resulting from the lack of APJ in ECs is prevented by LIF. (**A**) Effect on astrocyte GFAP positivity of medium conditioned by bEnd3 ECs stimulated with 50 ng/ml or 500 ng/ml apelin. Total RNA was extracted from dissociated retinal cells 24 hours after treatment with conditioned medium and qPCR analysis was performed to examine the expression of *Gfap* mRNA. $^{**}P<0.01$. (**B**) qPCR analysis of *Cntf* and *Lif* using RNA isolated from FACS-sorted PECAM1$^+$ ECs of P6 mouse retinas ($n=4$, $^*P<0.05$; N.S., not significant). (**C**) qPCR analysis of *LIF* mRNA expression in HUVECs. Total RNA was extracted from HUVECs stimulated with 50 ng/ml apelin for 0-12 hours ($n=3$, $^*P<0.05$). (**D-F**) Effects of LIF on aberrant outgrowth of ECs and astrocytes. (D) Retinas of P5 *APJ* KO mice were dissected 48 hours after intraocular injection of PBS or LIF and stained with antibodies against PDGFRα, GFAP and PECAM1. LIF inhibited astrocyte proliferation (surrounded by arrowheads) and induced upregulation of GFAP even ahead of the sprouting edge. Scale bar: 100 μm. (E) Quantitative evaluation of the number of PAX2$^+$ astrocytes in vascular or avascular areas of *APJ* KO retina after treatment with PBS or LIF ($n=3$, $^*P<0.05$). (F) qPCR analysis of *Vegfa* mRNA expression in sorted PDGFRα$^+$ cells of P5 PBS- or LIF-treated *APJ* KO retinas ($n=3$, $^*P<0.05$). Error bars indicate s.d.

acids. It is possible that apelin affects ECs that are continuously expressing APJ in the retina, not only locally but also in a wider context. While apelin in the retina has been reported to have proangiogenic properties (del Toro et al., 2010), we previously reported that it also acts as a maturation factor for newly developing blood vessels. It induces the assembly of ECs, and thus promotes the formation of larger blood vessels (Kidoya et al., 2008). It also stabilizes the junction protein VE-cadherin and thus inhibits vascular hyperpermeability induced by VEGF or inflammatory stimuli (Kidoya et al., 2010). Therefore, diverse functions for apelin during angiogenesis have been postulated. VEGF has strong proangiogenic activity, but also induces the production of vasohibin 1, which has anti-angiogenic activity (Watanabe et al., 2004). This implies that proangiogenic factors might also concurrently induce anti-angiogenic factors in ECs as part of a negative-feedback regulatory mechanism. LIF production from ECs upon activation of APJ might also be involved in such a negative-feedback system during angiogenesis. Based on the phenotype of *Apln* KO or *APJ* KO mice, we conclude that apelin facilitates angiogenesis by inducing proliferation of ECs, but subsequently indirectly finalizes angiogenesis by furthering the maturation of astrocytes in the retina. Therefore, delay of capillary outgrowth from the optic nerve head, and the suppression of vascular network formation, are primarily defects induced by the lack of APJ or apelin. The partial hypervascularity subsequently observed in the migrating front of the vascular network-forming area is, indirectly, a secondary deficit caused by insufficient maturation of astrocytes.

We previously reported that TIE2 activation by ANG1 in ECs is one pathway of apelin production (Kidoya et al., 2008). Consistent with ANG1 regulating the enlargement of blood vessels, we found that apelin also induces enlarged blood vessels by promoting the assembly of ECs. Based on these findings, we reported apelin as a factor for constructing enlarged blood vessels and that it acts as a downstream regulator of the ANG1/TIE2 system. We initially focused on enlargement of blood vessels in retinas from *APJ* KO mice. However, *APJ* KO mice showed moderate defects of vascular network formation in their retinas and we could not clearly compare vascular diameters because of delayed blood vessel formation in these mice.

ANG1 production is usually induced in mural cells, which are located beside both tip cells and stalk cells. With respect to mural cell localization, WT and *APJ* KO mice were indistinguishable (supplementary material Fig. S4). Therefore, ANG1 might affect both tip cells and stalk cells. Because apelin mRNA is expressed predominantly in tip cells in the retina (del Toro et al., 2010; Strasser et al., 2010), these might possess a specific machinery for apelin production, which could be affected by ANG1. However, mechanisms regulating apelin production in tip cells have not been elucidated. It has previously been reported that ANG1 is produced by astrocytes upon re-oxygenation after ischemia and has been suggested to play an important role in the barrier function associated with tight junction proteins (Lee et al., 2003). We previously reported that apelin also induces stabilization of VE-cadherin in ECs, as

described above (Kidoya et al., 2010). Therefore, further studies of the relationship between ANG1 and apelin and of the additional involvement of other mechanisms regulating apelin production in tip cells as influenced by mural cells or astrocytes are required.

In the brain, neural precursor cells (NPCs) generate neurons and subsequently glia. This switch is crucial for determination of the number of neurons and glia. Mechanisms regulating the differentiation of glia from NPCs, such as how and where the commitment to the glial lineage is made, have been extensively analyzed (Freeman, 2010; Rowitch and Kriegstein, 2010). However, regulation of astrocyte differentiation from immature to mature cells in vivo is not well characterized. One line of evidence suggests that oxygen levels control astrocyte differentiation, i.e. inadequate vascularity in the retina induces hypoxia, resulting in the suppression of astrocyte differentiation (West et al., 2005). Reciprocally, well-organized vascular formation triggers maturation of astrocytes under normoxia. Deficiency of APJ also induces hypoxia because of insufficient outgrowth of blood vessels; such hypoxia may then induce hypervascularity caused by VEGF upregulation and release from immature astrocytes. It is possible that maturation arrest of astrocytes might be secondary to the lack of APJ; however, we found that expression of LIF, an astrocyte maturation factor, is induced in ECs by stimulation with apelin. Because LIF expression is reduced in *APJ* KO mice, these data suggest that complex mechanisms, such as hypoxia and attenuation of LIF, underlie the suppression of astrocyte maturation in *APJ* KO mice.

Although it has been reported that LIF secreted by ECs induces astrocyte maturation (Kubota et al., 2008; Mi et al., 2001), how LIF is induced in ECs in vivo has not been determined. Our present data suggest that LIF production mediated by activation of APJ in ECs by apelin is one of the programmed processes regulating maturation of astrocytes in vivo, which facilitates well-organized vascular and astrocyte network formation in the retina. However, it has been reported that *Lif* KO mice show overall hypervascularity in their retinas (Kubota et al., 2008) and this phenotype is different from that of *APJ* KO mice because hypervascularity was restricted to the migrating front of the vascular network area in these latter mice. GFAP positivity in astrocytes at areas other than the migrating front of the vascular network did not differ between WT and *APJ* KO mice (Fig. 2A). This suggests the existence of mechanisms other than the apelin/APJ system for astrocyte maturation and indicates that further investigation is required to achieve a full understanding of the molecular mechanisms of blood vessel and astrocyte maturation.

Acknowledgements
Special thanks are due to Yoshiaki Kubota (Department of Cell Differentiation, Sakaguchi Laboratory, School of Medicine, Keio University, Shinjuku-ku, Tokyo, Japan) for outstanding technical support. We also thank Ping Xie for technical support and Keisho Fukuhara and Noriko Fujimoto for general assistance.

Funding
This work was partly supported by a grant from the Ministry of Education, Science, Sports, and Culture of Japan.

Competing interests statement
The authors declare no competing financial interests.

Supplementary material
Supplementary material available online at
http://dev.biologists.org/lookup/suppl/doi:10.1242/dev.072330/-/DC1

References

Augustin, H. G., Koh, G. Y., Thurston, G. and Alitalo, K. (2009). Control of vascular morphogenesis and homeostasis through the angiopoietin-Tie system. *Nat. Rev. Mol. Cell Biol.* **10**, 165-177.

Bonni, A., Sun, Y., Nadal-Vicens, M., Bhatt, A., Frank, D. A., Rozovsky, I., Stahl, N., Yancopoulos, G. D. and Greenberg, M. E. (1997). Regulation of gliogenesis in the central nervous system by the JAK-STAT signaling pathway. *Science* **278**, 477-483.

Chu, Y., Hughes, S. and Chan-Ling, T. (2001). Differentiation and migration of astrocyte precursor cells and astrocytes in human fetal retina: relevance to optic nerve coloboma. *FASEB J.* **15**, 2013-2015.

del Toro, R., Prahst, C., Mathivet, T., Siegfried, G., Kaminker, J. S., Larrivee, B., Breant, C., Duarte, A., Takakura, N., Fukamizu, A. et al. (2010). Identification and functional analysis of endothelial tip cell-enriched genes. *Blood* **116**, 4025-4033.

Freeman, M. R. (2010). Specification and morphogenesis of astrocytes. *Science* **330**, 774-778.

Fruttiger, M., Calver, A. R., Kruger, W. H., Mudhar, H. S., Michalovich, D., Takakura, N., Nishikawa, S. and Richardson, W. D. (1996). PDGF mediates a neuron-astrocyte interaction in the developing retina. *Neuron* **17**, 1117-1131.

Gariano, R. F. (2003). Cellular mechanisms in retinal vascular development. *Prog. Retin. Eye Res.* **22**, 295-306.

Gerhardt, H., Golding, M., Fruttiger, M., Ruhrberg, C., Lundkvist, A., Abramsson, A., Jeltsch, M., Mitchell, C., Alitalo, K., Shima, D. et al. (2003). VEGF guides angiogenic sprouting utilizing endothelial tip cell filopodia. *J. Cell Biol.* **161**, 1163-1177.

Ishida, J., Hashimoto, T., Hashimoto, Y., Nishiwaki, S., Iguchi, T., Harada, S., Sugaya, T., Matsuzaki, H., Yamamoto, R., Shiota, N. et al. (2004). Regulatory roles for APJ, a seven-transmembrane receptor related to angiotensin-type 1 receptor in blood pressure in vivo. *J. Biol. Chem.* **279**, 26274-26279.

Kasai, A., Shintani, N., Kato, H., Matsuda, S., Gomi, F., Haba, R., Hashimoto, H., Kakuda, M., Tano, Y. and Baba, A. (2008). Retardation of retinal vascular development in apelin-deficient mice. *Arterioscler. Thromb. Vasc. Biol.* **28**, 1717-1722.

Kidoya, H., Ueno, M., Yamada, Y., Mochizuki, N., Nakata, M., Yano, T., Fujii, R. and Takakura, N. (2008). Spatial and temporal role of the apelin/APJ system in the caliber size regulation of blood vessels during angiogenesis. *EMBO J.* **27**, 522-534.

Kidoya, H., Naito, H. and Takakura, N. (2010). Apelin induces enlarged and nonleaky blood vessels for functional recovery from ischemia. *Blood* **115**, 3166-3174.

Kishimoto, T., Akira, S., Narazaki, M. and Taga, T. (1995). Interleukin-6 family of cytokines and gp130. *Blood* **86**, 1243-1254.

Kubota, Y., Hirashima, M., Kishi, K., Stewart, C. L. and Suda, T. (2008). Leukemia inhibitory factor regulates microvessel density by modulating oxygen-dependent VEGF expression in mice. *J. Clin. Invest.* **118**, 2393-2403.

Kurihara, T., Kubota, Y., Ozawa, Y., Takubo, K., Noda, K., Simon, M. C., Johnson, R. S., Suematsu, M., Tsubota, K., Ishida, S. et al. (2010). von Hippel-Lindau protein regulates transition from the fetal to the adult circulatory system in retina. *Development* **137**, 1563-1571.

Lee, S. W., Kim, W. J., Choi, Y. K., Song, H. S., Son, M. J., Gelman, I. H., Kim, Y. J. and Kim, K. W. (2003). SSeCKS regulates angiogenesis and tight junction formation in blood-brain barrier. *Nat. Med.* **9**, 900-906.

Mi, H., Haeberle, H. and Barres, B. A. (2001). Induction of astrocyte differentiation by endothelial cells. *J. Neurosci.* **21**, 1538-1547.

Rowitch, D. H. and Kriegstein, A. R. (2010). Developmental genetics of vertebrate glial-cell specification. *Nature* **468**, 214-222.

Saint-Geniez, M., Argence, C. B., Knibiehler, B. and Audigier, Y. (2003). The msr/apj gene encoding the apelin receptor is an early and specific marker of the venous phenotype in the retinal vasculature. *Gene Expr. Patterns* **3**, 467-472.

Sato, T. N., Tozawa, Y., Deutsch, U., Wolburg-Buchholz, K., Fujiwara, Y., Gendron-Maguire, M., Gridley, T., Wolburg, H., Risau, W. and Qin, Y. (1995). Distinct roles of the receptor tyrosine kinases Tie-1 and Tie-2 in blood vessel formation. *Nature* **376**, 70-74.

Strasser, G. A., Kaminker, J. S. and Tessier-Lavigne, M. (2010). Microarray analysis of retinal endothelial tip cells identifies CXCR4 as a mediator of tip cell morphology and branching. *Blood* **115**, 5102-5110.

Suri, C., Jones, P. F., Patan, S., Bartunkova, S., Maisonpierre, P. C., Davis, S., Sato, T. N. and Yancopoulos, G. D. (1996). Requisite role of angiopoietin-1, a ligand for the TIE2 receptor, during embryonic angiogenesis. *Cell* **87**, 1171-1180.

Takakura, N., Watanabe, T., Suenobu, S., Yamada, Y., Noda, T., Ito, Y., Satake, M. and Suda, T. (2000). A role for hematopoietic stem cells in promoting angiogenesis. *Cell* **102**, 199-209.

Uemura, A., Kusuhara, S., Wiegand, S. J., Yu, R. T. and Nishikawa, S. (2006). Tlx acts as a proangiogenic switch by regulating extracellular assembly of fibronectin matrices in retinal astrocytes. *J. Clin. Invest.* **116**, 369-377.

Watanabe, K., Hasegawa, Y., Yamashita, H., Shimizu, K., Ding, Y., Abe, M., Ohta, H., Imagawa, K., Hojo, K., Maki, H. et al. (2004). Vasohibin as an endothelium-derived negative feedback regulator of angiogenesis. *J. Clin. Invest.* **114**, 898-907.

West, H., Richardson, W. D. and Fruttiger, M. (2005). Stabilization of the retinal vascular network by reciprocal feedback between blood vessels and astrocytes. *Development* **132**, 1855-1862.

Zhang, Y. and Stone, J. (1997). Role of astrocytes in the control of developing retinal vessels. *Invest. Ophthalmol. Vis. Sci.* **38**, 1653-1666.

Oncogene (2012) 31, 3254–3264

www.nature.com/onc

ORIGINAL ARTICLE

The apelin/APJ system induces maturation of the tumor vasculature and improves the efficiency of immune therapy

H Kidoya[1,4], N Kunii[2,3,4], H Naito[1], F Muramatsu[1], Y Okamoto[2], T Nakayama[3] and N Takakura[1]

[1]*Department of Signal Transduction, Research Institute for Microbial Diseases, Osaka University, Osaka, Japan;* [2]*Department of Otorhinolaryngology and Head and Neck Surgery, Graduate School of Medicine, Chiba University, Chiba, Japan and* [3]*Department of Immunology, Graduate School of Medicine, Chiba University, Chiba, Japan*

Immature and unstable tumor vasculature provides an aberrant tumor microenvironment and leads to resistance of tumors to conventional therapy. Hence, normalization of tumor vessels has been reported to improve the effect of immuno-, chemo- and radiation therapy. However, the humoral factors, which can effectively induce maturation of tumor vasculature, have not been elucidated. In this study, we found that the novel peptide apelin and its receptor APJ can induce the morphological and functional maturation of blood vessels in tumors. This apelin-induced tumor vascular maturation enhances the efficacy of cancer dendritic cell-based immunotherapy and significantly suppresses tumor growth by promoting the infiltration of invariant natural killer T cells into the central region of the tumor and thereby robustly inducing apoptosis of tumor cells. Additionally, we showed APJ expression to be enhanced in the tumor endothelium in comparison with normal-state endothelial cells. These findings provide a new target for tumor vascular-specific maturation, which is expected to improve the efficacy of conventional cancer therapies.

Oncogene (2012) **31**, 3254–3264; doi:10.1038/onc.2011.489; published online 31 October 2011

Keywords: tumor angiogenesis; immune therapy; vascular normalization; vascular maturation; apelin/APJ

Introduction

Agents targeting the tumor vasculature have been used for antitumor therapy in various preclinical and clinical studies (Gasparini *et al.*, 2005; Heath and Bicknell, 2009). The function of vascular endothelial growth factor (VEGF)-family ligands and their receptors in tumor angiogenesis has been well established, and serves as a logical target for antiangiogenic cancer therapy (Lohela *et al.*, 2009).The anti-VEGF monoclonal antibody, bevacizumab, neutralizes all isoforms of human VEGF (Gerber and Ferrara, 2005). Combining bevacizumab with chemotherapeutic agents appears to result in modest survival benefit in patients with metastatic colorectal cancer (Hurwitz *et al.*, 2004). This antitumor effect of bevacizumab was assumed to be due to its disruption of VEGF, and it was expected to directly suppress endothelial cell (EC) growth and inhibit tumor angiogenesis. However, Jain and co-workers recently showed that anti-angiogenic therapy causes 'normalization' of aberrant tumor vasculature and thus induces the formation of functional mature vasculature (Jain, 2005). This normalization of the tumor vasculature is effective for combination antitumor therapies, because mature vasculature and increased blood flow to tumors can promote the delivery of antitumor therapeutics to tumor cells (Dickson *et al.*, 2007). Therefore, investigating the role played by endogenous vascular maturation factors during the angiogenesis process could help in the development of a new antitumor therapy.

Apelin, a secreted peptide, has been identified as the endogenous ligand of the G-protein-coupled cell-surface receptor APJ (Tatemoto *et al.*, 1998). Apelin and APJ mediate a wide range of physiological actions, including angiogenesis (Cox *et al.*, 2006; Eyries *et al.*, 2008; Kasai *et al.*, 2008; Kidoya *et al.*, 2008), heart contractility, blood pressure regulation (Dai *et al.*, 2006) and other effects (Sorhede Winzell *et al.*, 2005; Lambrecht *et al.*, 2006; Lago *et al.*, 2007). Apelin and APJ are expressed on ECs of newly developing blood vessels during angiogenesis (Kidoya *et al.*, 2008), and it has been reported that apelin expression is induced by hypoxia in ECs (Eyries *et al.*, 2008). *In vitro* analyses revealed that apelin stimulates the proliferation, migration and tube formation of ECs (Kasai *et al.*, 2004; Masri *et al.*, 2004). Recently, we reported that apelin-deficient mice have narrow blood vessels, but in contrast, apelin-overexpressing mice have enlarged blood vessels. Apelin induces larger cords of ECs, mainly mediated by cell–cell aggregation, resulting in the formation of enlarged blood vessels (Kidoya *et al.*, 2008). These enlarged blood vessels are stable, and vascular permeability was reduced (Kidoya *et al.*, 2010). Taken together, these data support the notion that the apelin/APJ pathway has an important role in vascular maturation, especially for regulating the caliber of blood vessels to facilitate lumen enlargement (Kasai *et al.*, 2008; Kidoya *et al.*, 2008).

Correspondence: Professor N Takakura, Department of Signal Transduction, Research Institute for Microbial Diseases, Osaka University, 3-1 Yamada-oka, Suita, Osaka 565-0871, Japan.
E-mail: ntakaku@biken.osaka-u.ac.jp
[4]These authors contributed equally to this work.
Received 24 July 2011; revised 3 September 2011; accepted 19 September 2011; published online 31 October 2011

Invariant natural killer T (iNKT) cells are implicated in the control of autoimmunity (Singh *et al.*, 2001), resistance to tumors (Shin *et al.*, 2001; Smyth *et al.*, 2002) and protection against infectious agents (Kakimi *et al.*, 2000). The iNKT cells are characterized by the co-expression of natural killer (NK) receptor and T-cell receptor (TCR), which is encoded in humans by Vα24-JαQ gene segments and in mice by homologous Vα14-Jα281 sequences (Taniguchi *et al.*, 2003). iNKT cells are activated by a specific glycolipid antigen α-galactosylceramide (αGalCer) presented on CD1d (Kawano *et al.*, 1997; Brossay *et al.*, 1998; Spada *et al.*, 1998). Activated iNKT cells also induce cell death in tumor cells by the expression of a wide variety of cell death-inducing effector molecules, including perforin, Fas ligand and tumor necrosis factor-related apoptosis-inducing ligand, in a manner similar to other cytotoxic cells such as NK cells and CD8 cytotoxic T cells (Nieda *et al.*, 2001). Furthermore, activation of iNKT cells induces a rapid release of cytokines, including interleukin-4, interleukin-12 and interferon-γ (IFN-γ) (Smyth *et al.*, 2002).

We previously reported that intravenous injection of αGalCer-pulsed dendritic cells (DCs) induced the activation of murine iNKT cells *in vivo*, and eradicated established metastatic tumor foci in models of mouse liver and lung metastasis (Shin *et al.*, 2001). Based on these observations in murine models, several clinical trials of intravenous injection of αGalCer-pulsed DCs have been performed (Nieda *et al.*, 2001; Motohashi *et al.*, 2009). In these studies, the interventions had limited clinical efficacy in advanced cancer patients, although iNKT cell-specific systemic immune responses had been induced in a large population of the patients. We hypothesized that optimal delivery of effector cells to the target tissues is necessary to improve the efficacy of this immunotherapy. Therefore, we performed a clinical trial using intra-arterial infusion of activated iNKT cells for patients with advanced head and neck cancer (Kunii *et al.*, 2009), and a significant tumor reduction was observed in some patients after direct infusion of iNKT cells to the tumor-feeding arteries.

In the present study, we analyze the expression and function of the apelin–APJ system in the tumor vasculature and examined the therapeutic effects of apelin-mediated tumor vascular normalization. Moreover, we also studied the effects of combination therapy with tumor vascular normalization by apelin and cancer immunotherapy by activated DC transplantation in the mouse tumor model.

Results

Apelin and APJ are highly expressed in tumor ECs

We previously reported temporal expression of APJ in ECs during angiogenesis in embryos and during the process of recovery from ischemic states (Kidoya *et al.*, 2008, 2010). To determine whether apelin and APJ are expressed in a cell type-specific manner in ECs of tumor vessels, we evaluated the expression of vascular apelin and APJ in growing syngeneic mouse tumors by real-time PCR and immunohistochemical analyses. In real-time PCR analysis, we used CD31+ CD45− ECs obtained from the heart, skin or tumors of mice by fluorescence-activated cell sorting sorting. Compared with normal tissue ECs, APJ was more highly expressed in ECs from colon26 murine colon adenocarcinoma and Lewis lung carcinoma (LLC) (Figure 1a).

Immunohistochemical analysis of tumor tissue derived from colon26 murine colon cancer revealed that apelin and APJ are specifically expressed in the tumor vasculature (Figures 1b and c). Apelin and APJ expression was not observed in all tumor vessels, but about 13% of vessels were APJ-positive and about 27% of vessels were apelin-positive (Figure 1d). By analyzing the relationship between location or caliber of vessels and APJ expression, many APJ-positive ECs were observed in the large-caliber blood vessels in the peripheral region (Figure 1e). We also detected apelin and APJ protein expression in LLC tumor tissue blood vessels by immunohistochemical staining (Figures 1f and g). In these tumors, most ECs co-expressed apelin and APJ as reported previously (Kälin *et al.*, 2007) (data not shown). These data indicated that apelin and APJ are highly expressed in tumor blood vessels.

Apelin induces blood vessel enlargement in tumors and inhibits tumor growth

To analyze the effects of apelin on the morphology of blood vessels, we first observed the growth of blood vessels in tumors. Colon26 mouse colon cancer cells stably transfected with the apelin expression vector (Figure 2a) were inoculated under the skin of BALB/c mice to form tumors. Overexpression of apelin greatly inhibited the growth of colon26 tumors in all three cell lines derived from distinct clones (Figure 2b). In agreement with a previous report that apelin induced enlarged blood vessels in the dermis of apelin Tg mice (Kidoya *et al.*, 2010), the caliber of blood vessels observed in tumors formed by colon26 cells transduced with apelin was enlarged compared with control colon26 tumors (Figures 2c–e). This enlargement of tumor vessels is not dependent on tumor size, because the lumen size of the vessels was different even for tumors of the same volume (300 mm^3) (Supplementary Figure 1; day 8 for colon26/vector, day 10 for colon26/apelin). However, there is little difference between density of blood vessels in apelin-expressing tumor and control tumor (date not shown). Blood vessel enlargement by apelin was also observed in tumors developed from PC3 human prostate cancer cells (Figures 2f–h) and B16 mouse melanoma cells (data not shown). This indicated that the action of apelin on the change in the caliber of blood vessels is not a specific response to colon26 cells.

It is well known that the size of newly developed blood vessels is affected by mural cell adhesion to ECs during the maturation process of blood vessel formation (Gerhardt and Betsholtz, 2003). Usually, the blood vessels observed in tumors are not well covered with mural cells. In order to determine whether apelin is

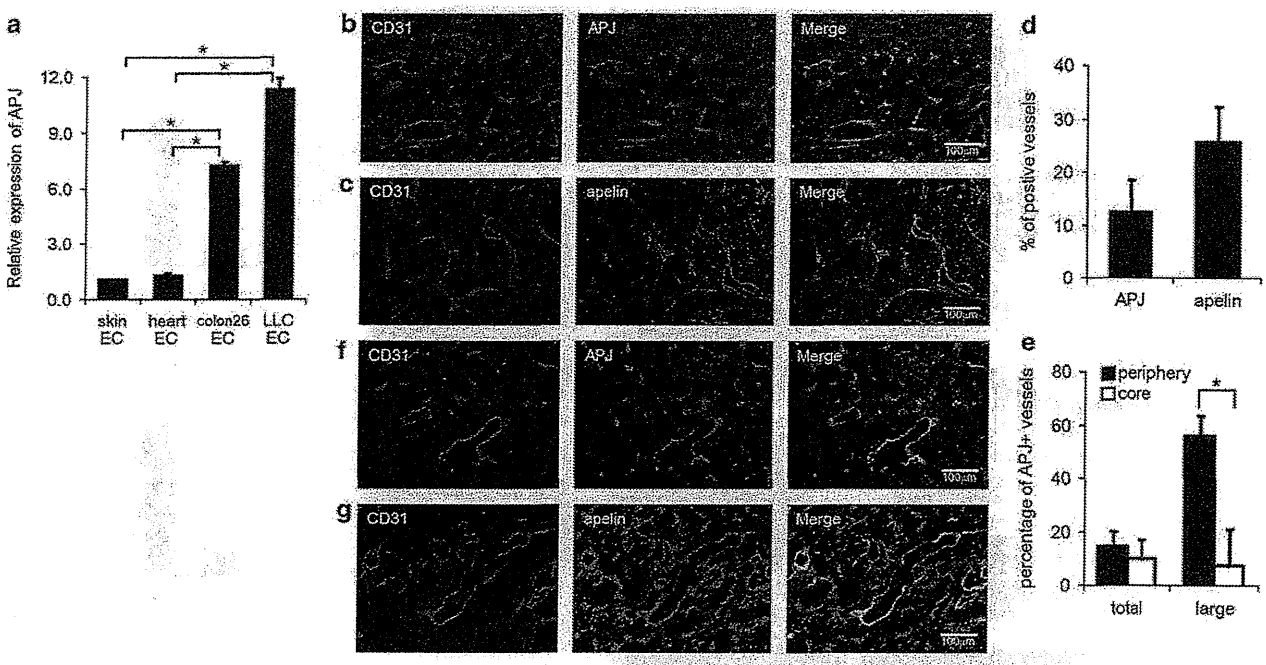

Figure 1 Analysis of apelin and APJ expression in ECs of the tumor vasculature. (**a**) Quantitative real-time PCR analysis of APJ mRNA expression in CD31+CD45− ECs derived from mouse skin and heart, and colon26 or LLC tumors 12 days after implantation. $*P<0.01$. (**b**, **c**) Immunohistochemical staining of sections from colon26 tumors using anti-CD31 (red) and anti-APJ (green) antibodies (**b**) or anti-apelin (green) antibodies (**c**). The scale bar indicates 100 μm. (**d**) Quantification of the ratio of tumor vessels expressing apelin or APJ. The data represent the ratio of apelin- or APJ-positive vessels versus apelin- or APJ-negative vessels as determined by immunohistochemical analysis. (**e**) Quantification of the size of APJ-positive blood vessels and their localization in colon26 tumors by immunohistochemical analysis. $*P<0.01$. (**f**, **g**) Immunohistochemical staining of tumor sections from LLC tumors using anti-CD31 (red) and anti-APJ (green) antibodies (**f**), or anti-apelin (green) antibodies (**g**). The scale bar indicates 100 μm.

involved in muscularization resulting in enlargement of blood vessels, tumor sections were stained with an anti-smooth muscle actin antibody. As shown in Figure 2i, the preexisting vessels around tumor were well muscularized, but mural cells did not adhere to the ECs of enlarged blood vessels in colon26 tumors expressing apelin. This suggested that the induced enlargement of blood vessels by apelin occurs independently of mural cells.

Apelin induces the formation of functional, non-leaky, mature vessels

Recent reports indicate that anti-angiogenic cancer therapy often converts the immature blood vessels in tumors to more a normal functional vascular network (Jain, 2005; Dickson *et al.*, 2007). As shown Figure 2b, apelin-mediated maturation of the tumor vasculature suppressed tumor growth. Therefore, we examined whether the apelin-induced enlargement of blood vessel also contributes to functional blood vessel normalization. Because the tumor vasculature is generally immature and leaky, oxygen cannot reach the center of the tumor tissue, leading to hypoxia. However, the hypoxic status of the center of tumor tissues was moderated in the tumors formed by the colon26 cells transduced with apelin (Figures 3a and b). Moreover, fluorescence-conjugated 100 mM dextran effectively infiltrated to the center of tumor tissues in apelin-expressing colon26 tumors (Figures 3c and d). These results indicate that the apelin-mediated enlargement of tumor vessels also induced the functional maturation of the blood vessels.

We then analyzed the phenotype of the CD31+CD45− ECs isolated from apelin-expressing or control colon26 tumors. In the apelin-transduced tumors, the expression level of EC-related genes VCAM1, Flk1, Flt1 and APJ was increased (Figures 3e and f). Furthermore, consistent with our previous report, expression of the EC junction proteins VE-cadherin and Claudin5 was upregulated (Figure 3f). Therefore, we speculated that the increased vascular stability observed in the apelin-expressing tumors is due to these changes in the EC phenotypes.

Functional analysis of αGalCer-pulsed mature BMDCs

Tumor vessel vascular normalization has been reported to enhance the therapeutic effects of anticancer drugs, radiotherapy and immunotherapy (Willett *et al.*, 2006). Therefore, we examined whether induction of functional normalization of blood vessels induced by apelin improved the efficacy of cancer immunotherapy. In addition, we hypothesized that vascular normalization would improve the migration of antitumor effector cells to the tumor site. Furthermore, we believed that

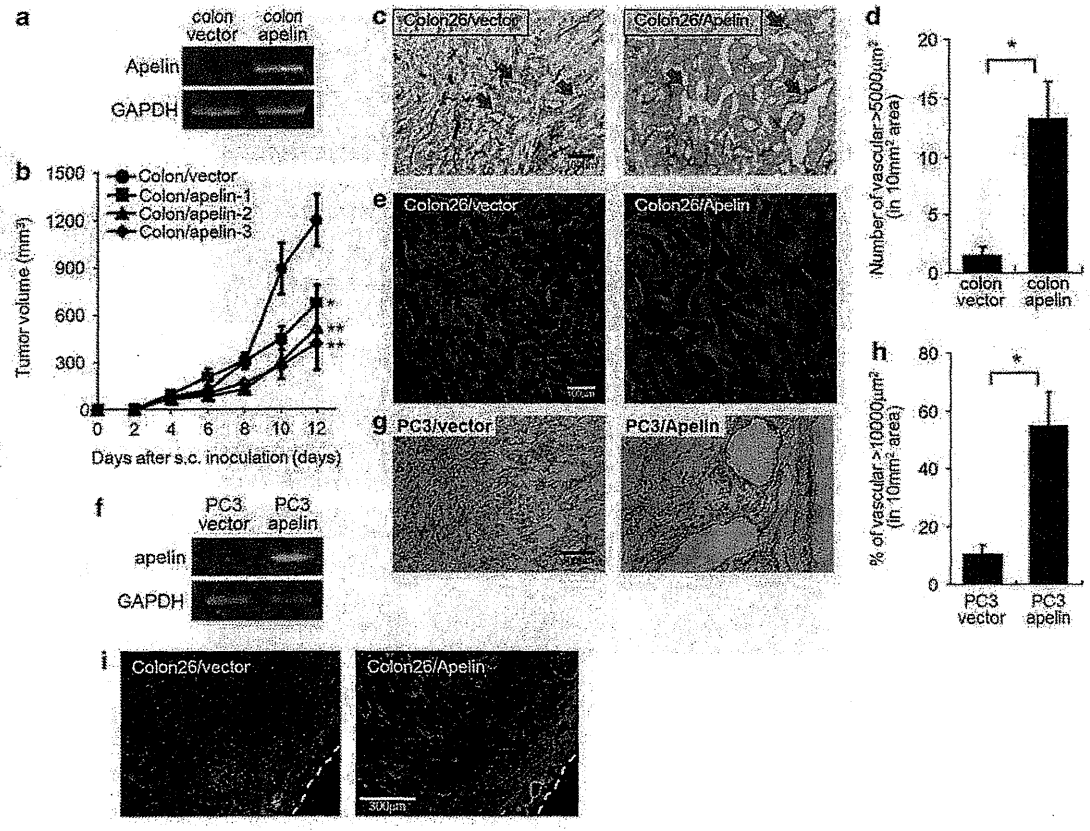

Figure 2 Apelin induces enlargement of blood vessels in tumors and inhibits tumor growth. (**a**) Reverse transcription–PCR (RT–PCR) analysis of apelin expression in colon26 tumor cells. GAPDH was used as a positive control. (**b**) The growth curves of control and apelin-overexpressing colon26 tumors implanted in the dorsa of BALB/c mice ($n=10$ mice per group). $^*P<0.05$; $^{**}P<0.01$ (comparison with colon/vector tumor). (**c**) Immunohistochemical staining of sections from tumors generated by colon26 cells and colon26 cells transduced with apelin. Blood vessels were stained by an anti-CD31 mAb (brown). The arrows indicate typical vessels. Scale bar, 100 μm. (**d**) The number of enlarged blood vessels having a $>5\times10^3$ μm² luminal cavity per 10-mm² area was quantitatively evaluated in each tumor section. $^*P<0.001$. (**e**) Confocal imaging of 50-μm sections from tumors generated from colon26 cells or colon26 cells transduced with apelin. Sections were stained by an anti-CD31 mAb. (**f**) RT–PCR analysis of apelin expression in PC3 tumor cells. GAPDH was used as a positive control. (**g**) Immunohistochemical staining of sections from tumors generated from PC3 cells or PC3 cells transduced with apelin. Sections were stained by an anti-CD31 mAb (brown). Scale bar, 100 μm. (**h**) The number of enlarged blood vessels having a $>10^4$ μm² luminal cavity per 10-mm² area was quantitatively evaluated in each tumor section. $^*P<0.001$. (**i**) Immunohistochemical staining of sections from control colon26 tumors or apelin-overexpressing colon26 tumors using an anti-CD31 antibody (green) and an anti-α-smooth muscle actin antibody (red). Scale bar, 300 μm.

effector cell-mediated cancer immunotherapy, combined with vascular normalization, would demonstrate more significant antitumor effects than either treatment alone.

iNKT cells are a very small cell population in the peripheral blood before stimulation with αGalCer, a specific glycolipid antigen (Kawano *et al.*, 1997; Brossay *et al.*, 1998; Spada *et al.*, 1998). After activation, the iNKT cell population significantly expands and exerts strong antitumor activity against various malignant tumors both *in vivo* and *in vitro* (Kawano *et al.*, 1999; Shin *et al.*, 2001; Seino *et al.*, 2005). Therefore, we investigated the synergistic effects between vascular normalization with apelin and immunotherapy with αGalCer-pulsed DCs whose antitumor response had already reported in mice and humans (Nieda *et al.*, 2004; Kunii *et al.*, 2009; Motohashi *et al.*, 2009).

Prepared αGalCer-pulsed or vehicle-pulsed mature bone marrow (BM)-derived DCs (BMDCs) were analyzed by flow cytometry after 8 days of culture. Both groups of BMDCs highly expressed CD11c (83%) and major histocompatibility complex (MHC) class-II (about 95%); moreover, the expression levels of CD86 and CD80 were also high (60–90%) (Figure 4a). These cells were injected into mice on day 0 and then the number of peripheral iNKT cells was monitored. The iNKT cell populations were significantly elevated on day 4 in mice injected with αGalCer-pulsed BMDCs (Figure 4b). Alternately, peripheral iNKT cell numbers remained at low levels in mice injected with vehicle-pulsed DCs. Therefore, we used both sets of DCs for antitumor immunotherapy experiments.

Enhancement of antitumor effects by combination of apelin stimulation and DC treatment

To evaluate the synergistic effect of apelin-mediated normalization of the tumor vasculature and immu-

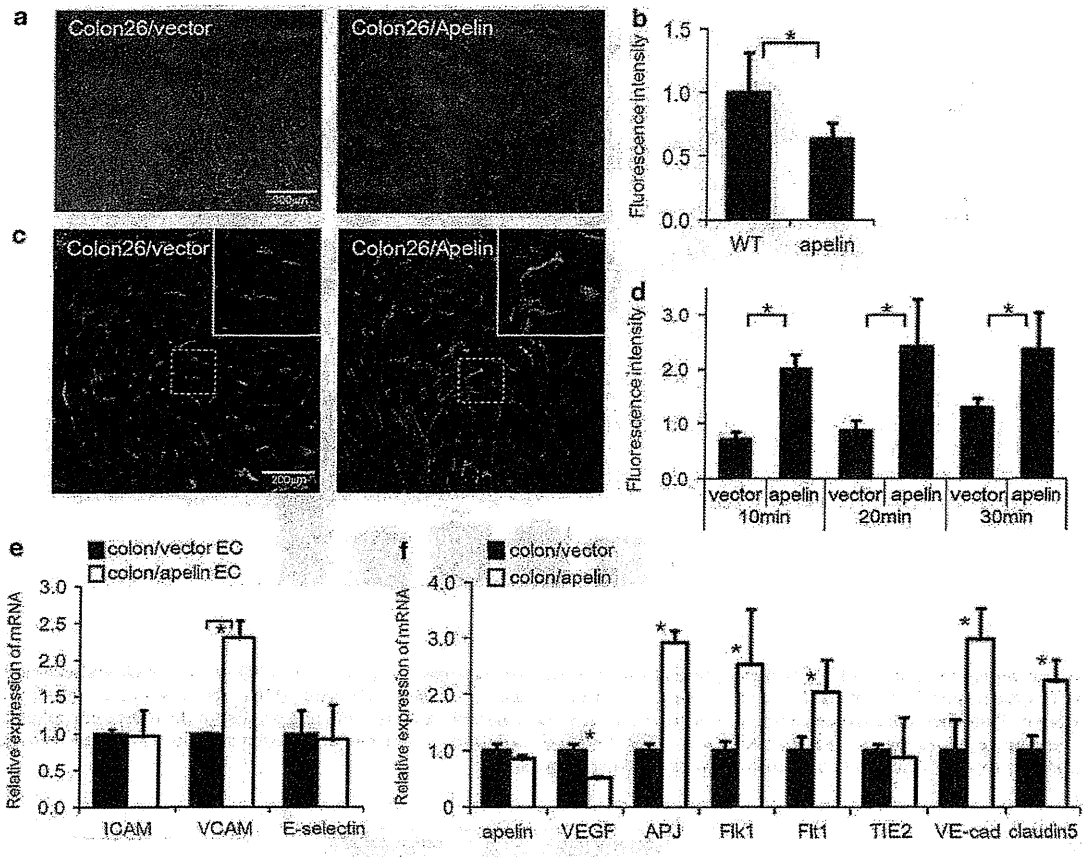

Figure 3 Apelin induces the formation of functional, non-leaky, mature vessels. (**a**) Colon26 control and apelin-overexpressing tumors were stained for CD31 (red) and hypoxia (HypoxyProbe, green). Scale bar, 100 μm. (**b**) The hypoxic region within the vascularized tumor was quantified by the fluorescence intensity in HypoxyProbe staining. $*P<0.01$. (**c**) Microscopy images of fluorescein isothiocyanate–dextran angiography and the vasculature (CD31, red) on colon26 control and apelin-overexpressing tumors. Scale bar, 100 μm. (**d**) Time-course analysis of the fluorescence intensity of extravascular fluorescein isothiocyanate–dextran as a measure of vascular permeability. $*P<0.01$. (**e**, **f**) Quantitative real-time RT–PCR analysis for cell adhesion molecules (**e**) or EC-related factors (**f**) using total RNA for CD31 + CD45− ECs isolated by cell sorting from colon26 control and apelin-overexpressing tumors. $*P<0.01$.

notherapy with mature DCs, we analyzed the antitumor activity of the combination therapy. Development of the tumor vasculature was observed between 4 and 6 days after implantation of colon26 cells (Supplementary Figure 2). Therefore, after implantation of colon26/vector or colon26/apelin cells into the subcutaneous tissue of mice, mature DCs were administered by intravenous injection on day 4 and tumors were harvested on day 14 (Figure 5a). We observed antitumor effects, as described previously, in the apelin-expressing tumor or in vector-transduced colon26 tumors treated with αGalCer/DCs, but more remarkable antitumor effects were observed in mice that underwent both apelin transduction and DC treatment (Figures 5b–d). Growth of colon26/apelin tumors treated with αGalCer/DCs slowed when tumor volumes exceeded 100 mm^3 (Figure 5b). The tumor weight of colon26/apelin tumors treated with αGalCer/DCs was exceedingly small and comprised only about a fourth of the vehicle/DCs-treated, apelin-transduced colon26 tumors or αGalCer/DCs-treated, vector-transduced colon26 tumors (Figures 5c and d). These data suggest that the vascular normalization induced by apelin markedly improved the effects of immunotherapy.

To exclude the possibility that apelin activated the immune cells and enhanced their antitumor effect, we analyzed the expression of APJ in iNKT cells and DCs. Compared with tumor blood vascular ECs, APJ expression in iNKT cells and in each of the DCs was extremely low and almost undetectable, respectively (Figure 5e). Therefore, apelin is not likely to directly activate these cells.

Infiltration of iNKT cells into tumor tissues was promoted by apelin-induced vascular maturation

Finally, to confirm that the antitumor effect observed in the colon26/apelin tumors treated with αGalCer/DCs was actually caused by iNKT cell infiltration into tumor tissue or activation induced by the DCs, we analyzed tumor tissues, which were harvested 14 days after tumor cell inoculation. We observed higher levels of NKp46 + cell infiltration in αGalCer/DC-treated colon26/apelin tumors as compared with colon/vector tumors and

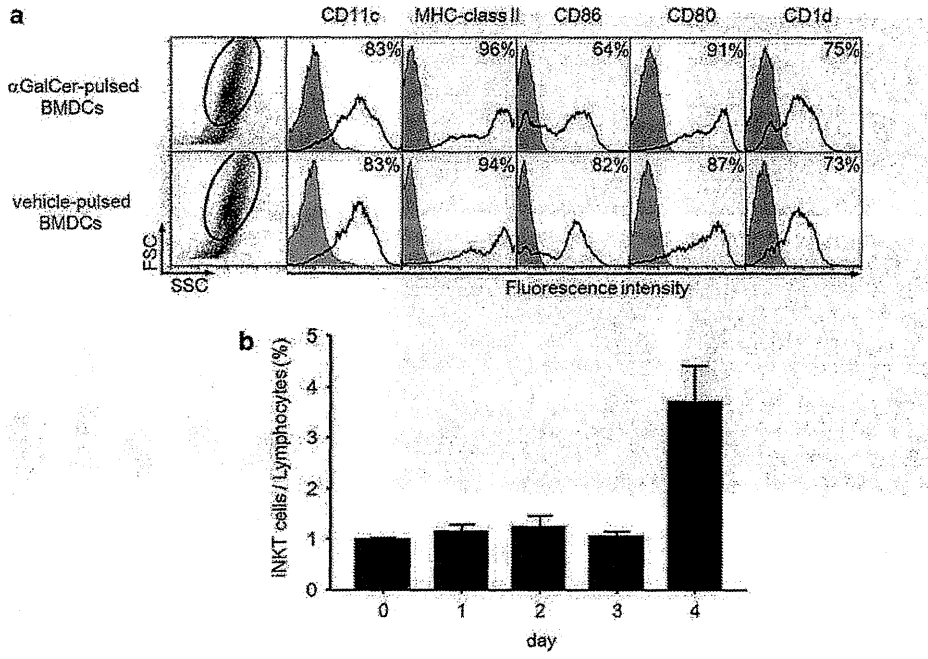

Figure 4 Functional analysis of αGalCer-pulsed mature BMDCs. (**a**) Flow-cytometric analysis of αGalCer- or vehicle-pulsed mature BMDCs. The expression levels of CD11c, human leukocyte antigen class-II, CD86, CD80 and CD1d were assessed at the time of administration. Thin lines: background staining with an isotype-matched control; bold line: staining profiles of the indicated molecules. (**b**) The percentage of peripheral blood iNKT cells (TCR-β + αGalCer-CD1d-tetramer + cells) after injection of αGalCer-pulsed mature BMDCs (6×10^5 cells) was assessed by flow-cytometric analysis.

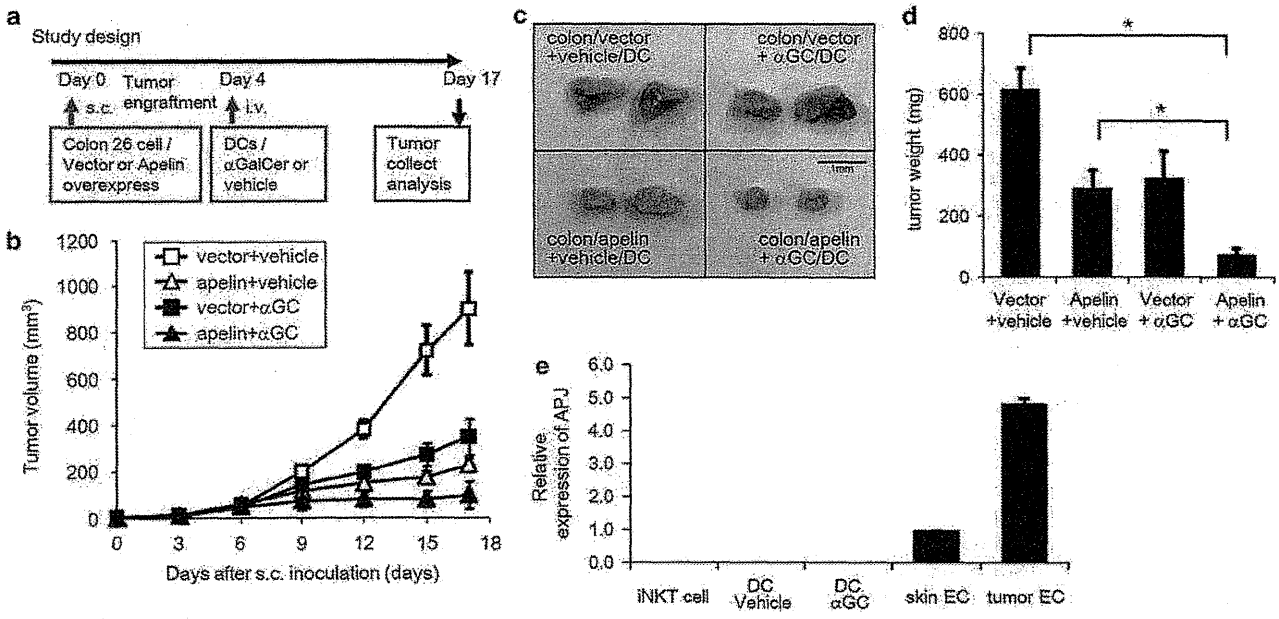

Figure 5 Enhancement of the antitumor effect by combination of apelin stimulation and DC treatment. (**a**) A schematic diagram of the experimental protocol of tumor isograft and DC treatment assays. (**b**) Growth curves of control and apelin-overexpressing colon26 tumors implanted in the dorsa of BALB/c mice treated with control vehicle-pulsed DCs or αGalCer-pulsed DCs ($n = 10$ mice per group). (**c**) Representative pictures of tumors collected 15 days after subcutaneous inoculation. Scale bar, 1 mm. (**d**) Tumor volume was determined on day 15 after subcutaneous inoculation of each tumor. $^*P < 0.01$. (**e**) Quantitative real-time RT–PCR analysis of APJ mRNA in iNKT cells and DCs. The results are shown as fold increase in comparison with the basal levels of normal ECs.

untreated tumors (Figure 6a). Consistent with this result, flow-cytometric analysis of αGalCer/DCs-treated colon/apelin tumors showed significant augmentation of iNKT cells (TCR-β + αGalCer-CD1d-tetramer +) in tumor tissues as compared with those in the untreated tumors (Figures 6b and c).

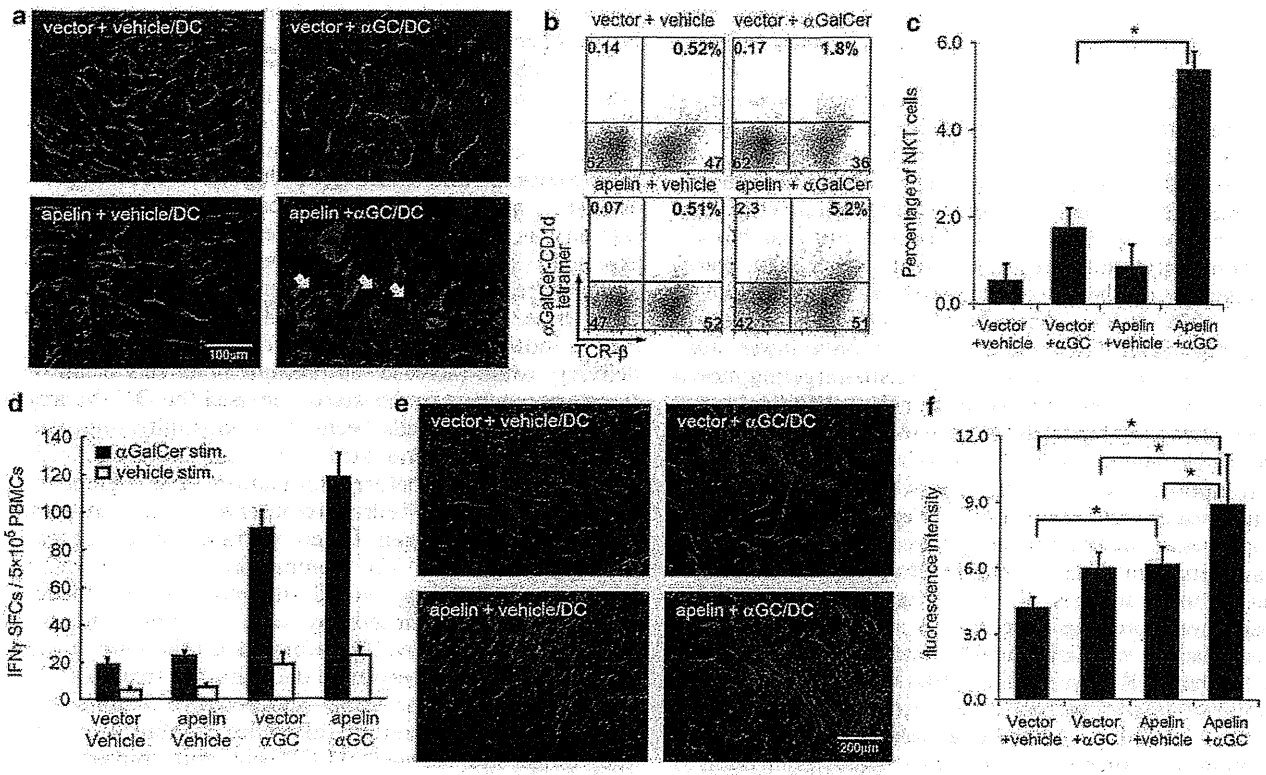

Figure 6 Infiltration of iNKT cells into tumor tissues was promoted by apelin-induced vascular maturation. (**a**) Immunohistochemical staining of sections from control and apelin-overexpressing colon26 tumors treated with control vehicle-pulsed DCs or αGalCer-pulsed DCs. Sections were stained by using anti-NKp46 (red) and anti-CD31 antibodies (green). Scale bar, 100 μm. (**b**) Flow-cytometric analysis of tumor-infiltrating CD45-positive lymphocytes. Cells were stained by a αGalCer-loaded CD1d tetramer and an anti-TCR-β antibody. (**c**) Quantitative evaluation of the percentage of iNKT cells (αGalCer-CD1d-tetramer + TCR-β + CD45 + iNKT cells/CD45 + lymphocytes) in tumor-infiltrating lymphocytes with s.d. $*P<0.01$. (**d**) The mean number of IFNγ spot-forming cells with s.d., determined by ELISpot assay. A total of 5×10^5 peripheral blood mononuclear cells were stimulated for 16 h with αGalCer or vehicle *in vitro*. The mean numbers of IFN-γ spots were determined from triplicate cultures. (**e**) Apoptosis of tumor cells was detected by the TUNEL method (green) and blood vessels were stained with an anti-CD31 antibody (red). Scale bar, 200 μm. (**f**) Quantification of apoptosis in tumor sections by measurement of fluorescence intensity of TUNEL-positive cells. $*P<0.01$.

IFN-γ production in response to αGalCer antigenic stimulation was increased in peripheral blood cells of mice treated with αGalCer/DCs (Figure 6d). Moreover, many apoptotic tumor cells were observed in αGalCer/DC-treated colon26/apelin tumors (Figures 6e and f). These results suggest that the potent antitumor effects observed in αGalCer/DC-treated colon26/apelin tumors was caused by enhanced infiltration of iNKT cells in the center of the tumor tissue, thus inducing apoptotic tumor cell death.

Discussion

We found that expression of APJ (the apelin receptor) was significantly increased in tumor blood vessels and apelin simulation induced enlargement of the caliber of tumor vessels. Enlargement of tumor vessels by apelin also led to functional maturation and normalization, including suppression of vascular permeability and improvement of oxygen supply to the central tumor.

Normalization of the tumor vasculature induced by VEGF-neutralizing antibodies has been reported to suppress tumor growth (Kim *et al.*, 1993). In our study, apelin-induced vascular maturation also demonstrated an antitumor growth effect. One of the major therapeutic benefits of tumor vascular normalization is enhancement of the effects of conventional cancer therapy such as chemotherapy, radiotherapy and immunotherapy. In our present study, we used a combination of immunotherapy with DC treatment with vascular normalization therapy due to apelin expression and obtained remarkable antitumor effects. These therapeutic effects resulted from induction of tumor cell apoptosis by effective infiltration of activated iNKT cells.

Several researchers have reported that apelin is relevant to blood vessel formation not only under physiological conditions, but also in a neoplastic context (Seaman *et al.*, 2007; Sorli *et al.*, 2007). Consistent with these results, we found that apelin expression was observed in vascular ECs of colon26 tumors and LLC tumors. In addition, we revealed that APJ expression was also upregulated in these tumor ECs. Our previous

report showed that APJ expression was induced by VEGF stimulation of ECs of blood vessels where angiogenesis is taking place (Kidoya *et al.*, 2008).We predict that APJ expression in tumor blood vessels is also regulated by the same mechanism, because angiogenesis is frequently observed in tumor tissues. Of interest, APJ-expressing angiogenic ECs are almost imperceptible in healthy adults. Although apelin has been reported to act on heart contractility and blood pressure regulation, apelin-deficient and apelin-overexpressing mice show normal growth after birth (Kidoya *et al.*, 2008, 2010). Therefore, anti-angiogenesis drugs targeting apelin would be expected to have fewer side effects than other anti-angiogenic agents targeting more ubiquitously expressed molecules such as VEGF.

We previously reported that apelin regulates the lumen size of the blood vessels of embryos during the vascular maturation process. In this report, we found that the tumor vasculature is also regulated by apelin stimulation. Blood vessels in tumors are functionally immature and characteristically leaky in nature (Bergers and Benjamin, 2003). From analysis of blood vessels in the skin of apelin-overexpressing mice, it was apparent that apelin can enhance vascular stability and suppress vascular permeability (Kidoya *et al.*, 2010). In the tumor vessels examined in our present study, we found that apelin improved stability and induced normalization by upregulating the expression of adhesion molecules in ECs.

Tumor blood vessels are structurally and functionally abnormal, and these abnormalities impair the tumor oxygen supply (Padera *et al.*, 2004). The hypoxic microenvironment formed in this manner induces genetic instability and leads to further alterations in malignant cells (Bottaro and Liotta, 2003). The vascular normalization induced by a VEGF-neutralizing antibody can alleviate the hypoxic condition of the tumor microenvironment and suppress malignant transformation. Apelin stimulation also improved the function of tumor blood vessels and alleviated the hypoxia. We attributed the growth suppression of the apelin-expressing tumors observed in this study to this effect. It is possible that tumor vessels normalized by apelin enhance the delivery of nutrients to tumor cells. However, this vascular normalization might also induce an antitumor effect by immunocyte infiltration, because the concentration of apoptotic tumor cells was increased in the colon/apelin + vehicle group as compared with the colon/vector + vehicle group, as shown in Figure 6f.

Contrary to our results, it has been reported that apelin induces tumor angiogenesis and promotes tumor growth (Sorli *et al.*, 2007). This difference might depend on the particular apelin–APJ signaling pathway that has been activated, such as the angiopietin1–Tie2 signaling pathway (Fukuhara *et al.*, 2008). The apelin–APJ system activates the Akt and ERK (extracellular-signal regulated kinase) signaling pathways, which might be involved in vascular stabilization and pro-angiogenesis, respectively. Therefore, apelin may have a beneficial effect in cancer treatment, if it can be predicted before treatment in individual cases that apelin induces normalization of the tumor vasculature.

Current immunotherapy for human solid cancers can be classified into the following categories (Rosenberg *et al.*, 2008): one is non-specific immunomodulation, such as interleukin-2 therapy for renal cancer or metastatic melanoma (Rosenberg *et al.*, 1989). Another is use of a cancer vaccine containing tumor peptides or DCs (Steinman and Banchereau, 2007) that activates the patient's immunity against their cancer. The last category is adoptive cell transfer, in which *in vitro* expanded autologous antitumor effector cells are administered to the patient (Rosenberg *et al.*, 2008). In all of these treatments, effector cell delivery to the tumor site is indispensable, and therefore, improvements in delivery would increase the therapeutic effects of all of these approaches. In this study, we used the DC therapy targeted to iNKT cells because tumor-infiltrating cells can be specifically evaluated. There are few iNKT cells at the tumor site before stimulation, and significant expansions of iNKT cells were observed after activation with the unique antigen. Based on these findings, it was strongly expected that combination with vascular normalization therapy would also improve the efficacy of the other immunotherapy such as tumor antigen-specific T-cell therapy. Therefore, as a follow-up study, we are preparing to examine combination treatment by adoptive cell transfer using engineered T lymphocytes (June *et al.*, 2009), and the difference in infiltration into the tumor site between iNKT cells and conventional T cells will be assessed.

Induction of vascular normalization leads to enhancement of the efficacy of conventional therapies (Willett *et al.*, 2006). Here we have demonstrated that combination therapy using vascular maturation induced by apelin and immune therapy with administration of antigen-loaded DCs remarkably suppressed the growth of colon26 tumors. This antitumor effect was attributed to dramatic infiltration of DC-activated iNKT cells and subsequent induction of apoptosis in the tumor cells. It was recently reported that inhibition of angiogenesis lead to normalized endothelial adhesion molecule levels and improves tumor growth inhibition by promoting leukocyte extravasation (Dings *et al.*, 2011). Upregulation of VCAM1 expression was also induced in the endothelium of apelin-expressing tumor, and it would promote iNKT cell infiltration. Tumor vascular normalization induced by apelin therefore appears to augment immunotherapy as well as chemotherapy and radiotherapy.

In summary, our data suggest that vascular normalization induced by apelin can enhance the effect of immunotherapy by promoting immune cell recruitment. Many angiogenic factors have been identified, and their functions have been described, and many of these factors have been or are being targeted as new cancer therapy approaches. Compared with these angiogenic molecules, apelin has a unique function in that it regulates blood vessel maturation, but has limited functions with regard to induction of angiogenesis. In addition, apelin-targeting agents would have fewer side effects, because expression of the apelin receptor, APJ, is confined to newly formed blood vessels such as tumor